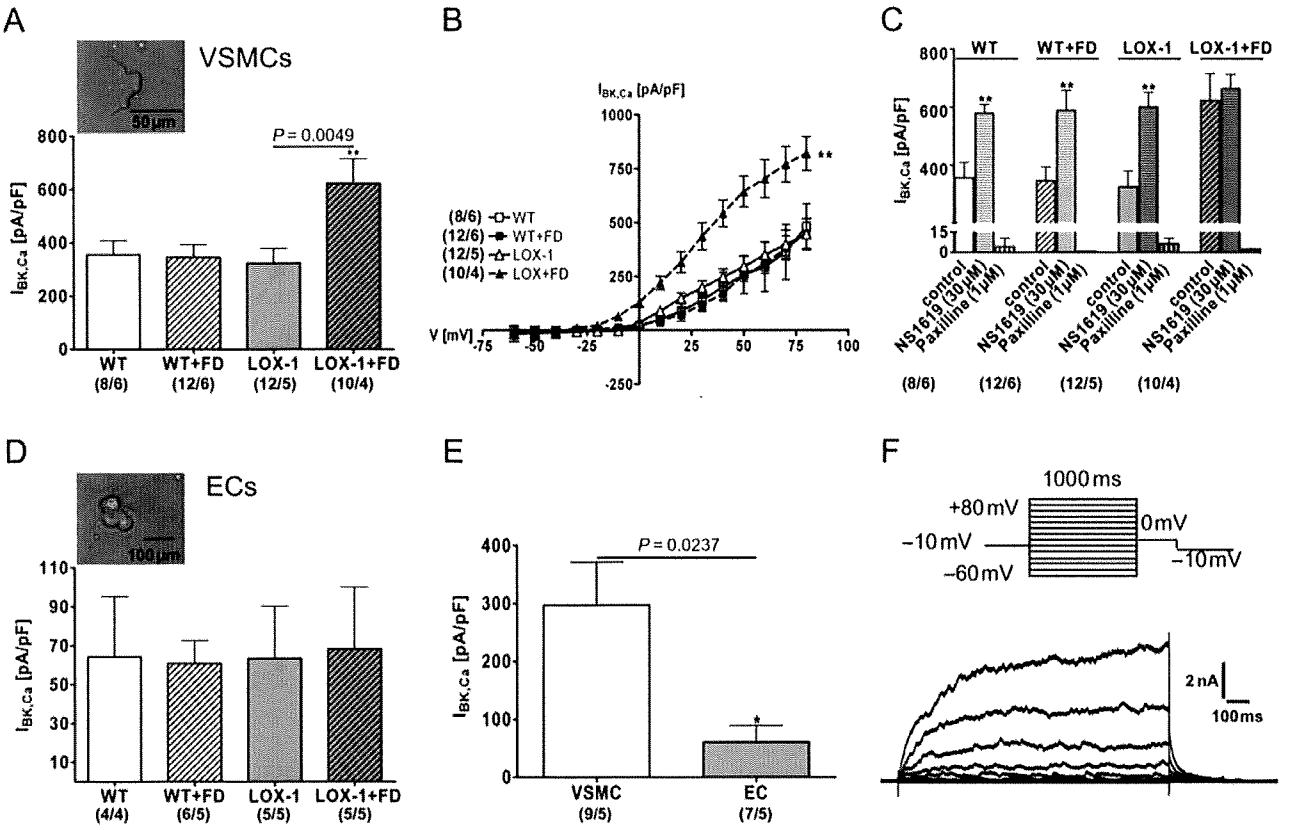

Figure 3 Characterization of electrophysiological properties in vascular smooth muscle cells (VSMCs) and endothelial cells (ECs) of mesenteric arteries from WT and LOX-1 mice on standard and high-fat diet. (*A*) Current density in pA/pF of BK_{Ca} currents in VSMCs from WT, WT + FD, LOX-1, and LOX-1 + FD. (*B*) Current-voltage relationships of BK_{Ca} currents of VSMC from WT, WT + FD, LOX-1, and LOX-1 + FD. $^{**}P < 0.01$ standard diet vs. high-fat diet. (*C*) Current density in pA/pF of BK_{Ca} channels in VSMCs in response to clamp steps to + 60 mV under control condition, with NS1619 (30 µmol/L) and paxilline (1 µmol/L) in WT, WT + FD, LOX-1, and LOX-1 + FD. Please note the different scaling factors for the ordinate. $^{**}P < 0.01$ control vs. NS1619. (*D*) Current density in pA/pF of BK_{Ca} channels in ECs from WT, WT + FD, LOX-1, and LOX-1 + FD. (*E*) Comparison of the BK_{Ca} currents in VSMCs and ECs from WT. (*F*) (Above) Pulse protocol; (Below) Typical BK_{Ca} current tracings of a VSMC from WT.

was even higher in LOX-1 + FD than in WT + FD animals (see Supplementary material online, *Figure S4*). We have also determined superoxide anions, because this particular fraction of ROS has been previously shown to result in H_2O_2 formation and act directly as an EDHF component.[32] We found that H_2O_2 levels were significantly increased in LOX-1 + FD mice (56.2 ± 5.8%) compared with the other groups (WT: 33.2 ± 3.4%; WT + FD: 40.6 ± 8.3%; LOX-1: 39.8 ± 5.7%; see Supplementary material online, *Figure S4*).

3.4 BK_{Ca} currents

Our results provide evidence that EDHF formation is involved in the contractile responses and that EDHF has the largest impact in the LOX-1 + FD group. Since EDHF activates BK_{Ca} channels, we measured BK_{Ca} currents in smooth muscle and ECs in order to elucidate their contribution to the observed EDHF-mediated response in LOX-1 + FD mice.

All VSMCs exhibited robust BK_{Ca} currents. The current amplitude was completely suppressed by the selective BK_{Ca} channel-blocker paxilline (1 µmol/L).[33] Current densities of $I_{BK,Ca}$ in VSMCs at a test potential of +60 mV were significantly higher in LOX-1 + FD mice (623 ± 93 pA/pF) compared with WT (356 ± 54 pA/pF), WT + FD (346 ± 47 pA/pF), and LOX-1 (324 ± 54 pA/pF; *Figure 3A* and *B*). In LOX-1 + FD $I_{BK,Ca}$ voltage dependence was shifted to lower voltages suggesting that the current is already activated at more negative potentials. Moreover, opening of BK_{Ca}-channels with the selective channel activator NS1619 (30 µmol/L)[34] did not further increase current density in LOX-1 + FD mice, but increased the current in the other groups to almost the same levels as previously observed in LOX-1 + FD (*Figure 3C*). Interestingly, the $I_{BK,Ca}$ current densities in ECs were similar in all four mice groups (WT: 64 ± 31 pA/pF; WT + FD: 61 ± 12 pA/pF; LOX-1: 63 ± 27 pA/pF; LOX-1 + FD: 68 ± 32 pA/pF), but much smaller than in VSMCs (*Figure 3D* and *E*). Next, we examined the effects of three supposed EDHFs, i.e. H_2O_2, 11,12-EET, and 14,15-EET, on BK_{Ca} channel activity in WT mice. At + 60 mV H_2O_2 (1 µmol/L) significantly increased current density, but not to the same value as observed with NS1619 or in LOX-1 + FD mice. 11,12-EET and 14,15-EET (300 nmol/L each) activated $I_{BK,Ca}$ to the same maximum as NS1619 (*Figure 4A–C*) in WT mice and as the observed amplitude in LOX-1 + FD animals.

3.5 mRNA expression of BK_{Ca} channel subunits and eNOS

Differences in current densities could be due to different expression levels of the relevant channel subunits. Therefore, we have measured mRNA expression of the BK_{Ca}-channels using real-time PCR (*Figure 5A* and *B*). Both the pore-forming α-subunits and the accessory β1-subunits

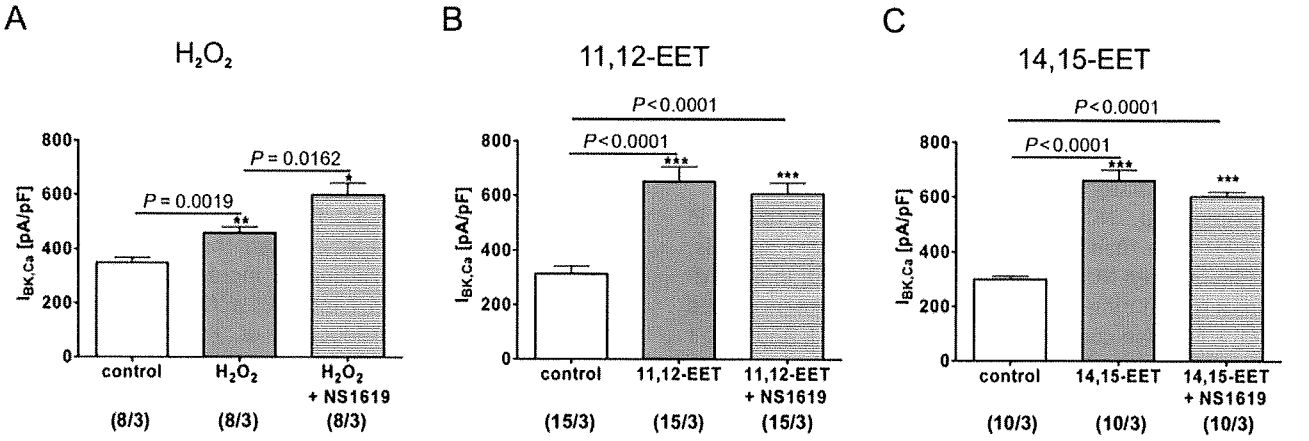

Figure 4 EDHF-mediated activation of BK_{Ca} currents in vascular smooth muscle cells (VMSCs) of mesenteric arteries from WT. (*A*) Hydrogen peroxide (1 μmol/L) activated the BK_{Ca} currents in VSMCs from WT, and even further increased with additional NS1619 (30 μmol/L). (*B*) 11,12-EET (300 nmol/L) significantly activated BK_{Ca} currents in VSMCs from WT to the same maximum like NS1619 (30 μmol/L). (*C*) Activation of BK_{Ca} currents by 14,15-EET (300 nmol/L) in VSMCs from WT to the similar values like NS1619 (30 μmol/L).

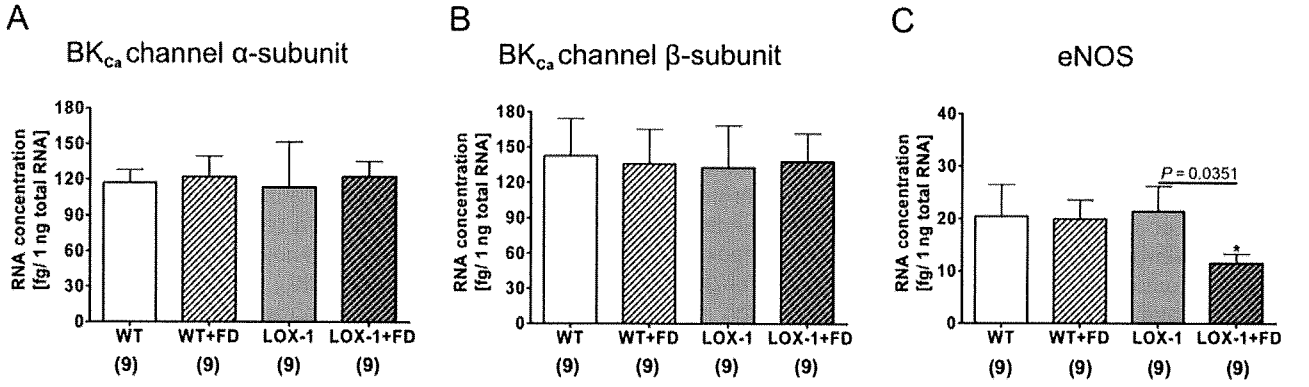

Figure 5 Expression of BK_{Ca} channel subunits and eNOS in mesenteric arteries. (*A*) BK_{Ca} channel α-subunit (KCNMA) mRNA expression was analysed by real-time PCR using an internal standard. (*B*) Amount of BK_{Ca} channel β_1-subunit (KCNMB1) mRNA was quantified by real-time PCR using an internal standard. (*C*) Expression of eNOS mRNA determined by real-time PCR using an internal standard. WT, wild-type; LOX-1, mice overexpressing LOX-1; FD, high-fat diet.

were expressed in similar amounts in all groups. In contrast mRNA expression of eNOS was lower in LOX-1 + FD mice compared with WT, WT + FD, and LOX-1 animals (*Figure 5C*). This finding is in agreement with the reduced NO-dependent vascular relaxation in this group of animals. In heart and kidney, we did not detect statistically significant differences in the mRNA and protein expression of the BK_{Ca} channel α- and β1-subunits and eNOS between all groups.

4. Discussion

The main findings of our study show that mice overexpressing the LOX-1 in combination with FD have markedly increased body weight, display impaired NO-mediated, and enhanced EDHF-dependent relaxation in mesenteric arteries, and have increased vascular ROS production in LOX-1 + FD compared with WT + FD animals. Furthermore, BK_{Ca} channel activity in VSMCs was higher in LOX-1 + FD, which could be increased by the EDHFs H_2O_2 and EETs. In contrast, endothelial BK_{Ca} channel activity was unchanged.

4.1 Body weight and plasma lipids

As expected, WT and LOX-1 overexpressing mice gained weight after FD. However, LOX-1 mice on standard diet were also heavier than their corresponding WT animals suggesting an impact of LOX-1 on weight control or metabolic status. Higher body weight in LOX-1 mice was not associated with a significant shift in plasma lipid parameters to a more harmful lipid profile as observed with FD in both WT and LOX-1 mice. In the latter two groups, elevated total plasma cholesterol, LDL, and HDL are in agreement with previous studies.[35,36] Furthermore the LDL/HDL quotient shifted to higher values suggesting an enhanced risk for endothelial dysfunction and atherosclerosis.[37]

4.2 Vascular constriction and relaxation

None of the animals had grossly visible atherosclerotic lesions. Therefore, we tested for vascular dysfunction as an early sign of cardiovascular disease by measuring contraction and endothelium-dependent as well as endothelium-independent relaxation of PE-preconstricted small resistance arterioles. The impact of oxLDL on vascular tone is not fully resolved. OxLDL enhances the basal tone in rabbit cerebral arteries.[38] In contrast, oxLDL has no effect on basal tone in rabbit aorta.[39] We observed no differences in basal vascular tone in the animal groups fed standard or FD. However, the maximum contractile response to PE was lower in LOX-1 + FD than in the other animals, but potencies

were similar. This difference in the vessel contraction between LOX-1 + FD mice and the other three animal groups was not observed in the presence of high, depolarizing potassium concentration or by the combination of PE and paxilline, suggesting a mechanism that involves potassium channel activity. BK_{Ca} channels also participate in ACh-/endothelium-mediated relaxation.[21-23]

ACh-stimulated, NO-mediated dilatation was lower in LOX-1 + FD mice than in WT, WT + FD, and LOX-1 animals, suggesting reduced NO availability in LOX-1 + FD. In accordance basal tone during L-NAME incubation was less increased in LOX-1 + FD mice compared with WT, WT + FD, and LOX-1 animals. Effectivity of L-NAME to eliminate NO production has been questioned because in some species, especially in pig and rabbit, endothelium-dependent/NO-mediated relaxation was resistant to eNOS-inhibitors.[40] In our experiments with mouse mesenteric arteries, however, relaxation persisting after inhibition of eNOS with L-NAME was fully suppressed with apamin and charybdotoxin, the combination of which is commonly used for EDHF block (data not shown). Possible explanations for decreased NO-mediated relaxation in mesenteric arteries of LOX-1 + FD mice are (i) that ROS production is elevated, (ii) that expression of eNOS mRNA is reduced, and (iii) that EDHF can compensate for the loss of NO.[41] In contrast to the reduced NO-mediated relaxation, the EDHF-dependent response was elevated in LOX-1 + FD mice compared with WT, WT + FD, and LOX-1 animals, but could be abolished by a general cytochrome P450 blocker or by an epoxygenase inhibitor. This finding suggests a potential role of cytochrome P450 and its epoxygenases as a compensatory mechanism that makes up for the loss of NO and subsequent endothelial dysfunction in LOX-1 + FD mice. This same amount of EDHF, which was abolished by the cytochrome P450 inhibitors, was also blocked by paxilline in the presence and absence of L-NAME suggesting an essential role of the BK_{Ca} channel in the EDHF-mediated relaxation. Block of cytochrome P450 or BK_{Ca} channels in LOX-1 + FD led to similar levels of persisting EDHF-mediated relaxation in all four groups. The nature of the persisting EDHF-mediated relaxation was not investigated in this study. As reported before, release of EDHF from ECs is associated with the endothelial activity of calcium-activated potassium channels of small and intermediate conductance,[21] but the activation of BK_{Ca} channels is involved in the EDHF-mediated relaxation of VSMCs. No relevant differences in endothelium-independent relaxation were detected, i.e. potency and efficacy of SNP were similar in all groups, suggesting comparable properties of VSMC-relaxation in mice on FD and standard diet. Interestingly, an EETs-mediated relaxation in response to 11,12-EET and 14,15-EET was significantly increased in mesenteric arteries with and without endothelium of LOX-1 + FD mice compared with WT, WT + FD, and LOX-1 animals (see Supplementary material online, *Figure S5*). This could be mediated by the compensatory enhanced activity of the BK_{Ca} channels in VSMCs of LOX-1 + FD mice. However, activation is not sufficient to compensate for the loss of NO in the LOX-1 + FD mice.

4.3 Vascular reactive oxygen species productions

Our results and several previous studies have shown that hypercholesterolaemia is associated with impaired endothelium-dependent relaxation in experimental and clinical studies.[1,42-44] Rapid degradation of endothelium-derived NO by high levels of ROS is thought to be a major mechanism underlying impaired endothelium-dependent vasodilatation under hypercholesterolaemic conditions. It should also be responsible for decreased endothelium-dependent relaxation.[45,46] In our experiments, ROS was indeed increased in LOX-1 + FD and WT + FD mice, and to a larger extent in the former than the latter. ROS leads to oxidation of LDL resulting in increased oxLDL levels. Uptake of oxLDL via LOX-1 into ECs activates NAD(P)H oxidases and enhances production of ROS,[47,48] starting a vicious cycle finally leading to endothelial dysfunction. However, exaggerated ROS production has not only deleterious effects. Growing evidence supports an import role of redox-sensitive signalling in vascular function.[49] Furthermore Shimokawa and Matoba[32] have suggested that the ROS product H_2O_2 could act as EDHF. H_2O_2 amount was higher in LOX-1 + FD mice than in WT, WT + FD, and LOX-1 animals, suggesting a potential role in the elevated EDHF-mediated relaxation.

4.4 Role of endothelium-derived hyperpolarizing factor and BK_{Ca} channel activity

In contrast to reduced NO-mediated responses, EDHF-mediated relaxation was most pronounced in LOX-1 + FD mice suggesting that this mechanism might partly compensate the impaired NO-mediated relaxation. Since different EDHFs, like EETs and H_2O_2 are known to activate BK_{Ca} channels in VSMCs,[21] we studied BK_{Ca} currents directly. At any activating potential, the amplitude of $I_{BK,Ca}$ was indeed larger in VSMCs from LOX-1 + FD than in the other groups. Moreover, $I_{BK,Ca}$ amplitude in LOX-1 + FD mice could not be further increased by the BK_{Ca} channel opener NS1619, suggesting that increased current amplitude resulted from enhanced channel open probability. This interpretation is supported by the fact that mRNA expression of the BK_{Ca} channel α- and β1-subunits was similar in all mice. Because of the limited availability of vascular tissue from the mesenteric arteries, no additional data on protein level could be obtained. However, similar mRNA and protein expression of BK_{Ca} channels have been demonstrated in human arteries and veins.[50] The $I_{BK,Ca}$ amplitudes in ECs were smaller than in VSMCs and did not reveal any differences between the four groups. Therefore BK_{Ca} channels in ECs do not contribute to vascular dysfunction in LOX-1 + FD mice. The activation of endothelial BK_{Ca}-channels contributes to the EDHF-mediated relaxation. Endothelial hyperpolarization can be transmitted directly via gap junctions to the VSMCs.[51,52] In addition, the K^+ outward current through BK_{Ca} channels increases the extracellular potassium concentration.[53] The subsequent activation of the inward-rectifier potassium channel (K_{IR}) and the Na^+/K^+ pump overcomes the minor depolarizing effects linked to the K^+ increase[54,55] and relaxes smooth muscle cells.

The possible EDHF H_2O_2 significantly increased $I_{BK,Ca}$ in VSMCs, although the level did not reach the maximum current amplitude of NS1619 or as in LOX-1 + FD mice. Therefore, H_2O_2 plays only a minor compensatory role in EDHF-mediated relaxation of this model. Recently, an inhibiting effect of H_2O_2 on cytochrome P450 has been

suggested, indicating a negative feedback mechanism of EET production.[56] This could not be confirmed in our experimental model.

Reduced NO levels have been reported to disinhibit cytochrome P450 and hence elevate two other possible EDHF components, 11,12-EET and 14,15-EET.[57–59] These two EETs were able to enhance $I_{BK,Ca}$ to similar maximum current amplitude as observed in the presence of NS1619 and in LOX-1 + FD. In agreement with previous findings in isolated renal arteries of hypercholesterolaemic rabbits,[18,19] we suggest that enhanced formation of EDHF represents a compensatory mechanism of the decreased NO-mediated vessel relaxation. In contrast, Urakami-Harasawa *et al.*[60] found a significant inhibition of endothelium-dependent hyperpolarization in isolated gastroepiploic arteries from atherosclerotic patients. These contradictory results could be explained by the longer duration of hypercholesterolaemic conditions and the progressive development of vascular diseases.

In the last few years, vascular BK_{Ca} channels were considered as potential therapeutic targets in the treatment of hypertension, endothelial dysfunction, and other cardiovascular diseases,[61] because aldosterone overexpression induces a nitric-oxide-independent coronary dysfunction with decreased VSMC BK_{Ca} expression and coronary BK_{Ca}-dependent relaxation.[62] However activation of LOX-1 in clinical manifestation of atherosclerosis could activate VSMC BK_{Ca} channels. In contrast, enhanced LOX-1 expression does not influence endothelial BK_{Ca} channels.

In conclusion, we have consistently detected significant changes in contractile and electrophysiological properties of small resistance vessels only in the combination of LOX-1 overexpression and FD. The endothelium-mediated relaxation via NO release was impaired, but partly compensated by the higher release of EDHF. The consequence of this compensatory mechanism was a higher $I_{BK,Ca}$ due to increased open probability of BK_{Ca} channels in VSMCs, but not in ECs. Our results clearly demonstrate that LOX-1 overexpression and FD cause functional changes in ECs and VSMCs of small resistance arteries leading to vascular dysfunction as an early sign of cardiovascular diseases.

Supplementary material

Supplementary material is available at *Cardiovascular Research* online.

Acknowledgements

The authors would like to thank Dr Melinda Wuest for helpful discussion and Claudia Bodenstein for excellent technical assistance.

Conflict of interest: none declared.

Funding

This work was supported by the German Federal Ministry of Education and Research and the Dr. Robert Pfleger foundation.

References

1. Simionescu M. Implications of early structural-functional changes in the endothelium for vascular disease. *Arterioscler Thromb Vasc Biol* 2007; **27**:266–274.
2. Brevetti G, Schiano V, Chiariello M. Endothelial dysfunction: a key to the pathophysiology and natural history of peripheral arterial disease? *Atherosclerosis* 2008;**197**:1–11.
3. Doan AC, Meller N, McNamara CA. Role of smooth muscle cells in the initiation and early progression of atherosclerosis. *Arterioscler Thromb Vasc Biol* 2008;**28**:812–819.
4. Abularrage CJ, Sidawy AN, Aidinian G, Singh N, Weiswasser JM, Arora S. Evaluation of the microcirculation in vascular disease. *J Vasc Surg* 2005;**42**:574–581.
5. Vohra RS, Murphy JE, Walker JH, Ponnambalam S, Homer-Vanniasinkam S. Atherosclerosis and the Lectin-like OXidized low-density lipoprotein scavenger receptor. *Trends Cardiovasc Med* 2006;**16**:60–64.
6. Chen XP, Zhang TT, Du GH. Lectin-like oxidized low-density lipoprotein receptor-1, a new promising target for the therapy of atherosclerosis? *Cardiovasc Drug Rev* 2007;**25**:146–161.
7. Morawietz H. LOX-1 and atherosclerosis: proof of concept in LOX-1-knockout mice. *Circ Res* 2007;**100**:1534–1536.
8. Sawamura T, Kume N, Aoyama T, Moriwaki H, Hoshikawa H, Aiba Y *et al.* An endothelial receptor for oxidized low-density lipoprotein. *Nature* 1997;**386**:73–77.
9. Draude G, Hrboticky N, Lorenz RL. The expression of the lectin-like oxidized low-density lipoprotein receptor (LOX-1) on human vascular smooth muscle cells and monocytes and its down-regulation by lovastatin. *Biochem Pharmacol* 1999;**75**:383–386.
10. Mehta JL, Chen J, Hermonat PL, Romeo F, Novelli G. Lectin-like, oxidized low-density lipoprotein receptor-1 (LOX-1): a critical player in the development of atherosclerosis and related disorders. *Cardiovasc Res* 2006;**69**: 36–45.
11. Tatsuguchi M, Furutani M, Hinagata J, Tanaka T, Furutani Y, Imamura S *et al.* Oxidized LDL receptor gene (OLR1) is associated with the risk of myocardial infarction. *Biochem Biophys Res Commun* 2003;**303**:247–250.
12. Hattori H, Sonoda A, Sato H, Ito D, Tanahashi N, Murata M *et al.* G501C polymorphism of oxidized LDL receptor gene (OLR1) and ischemic stroke. *Brain Res* 2006;**1121**:246–249.
13. Kataoka H, Kume N, Miyamoto S, Minami M, Moriwaki H, Murase T *et al.* Expression of the lectin like oxidized low-density lipoprotein receptor-1 in human atherosclerotic lesions. *Circulation* 1999;**99**:3110–3117.
14. Inoue K, Arai Y, Kurihara H, Kita T, Sawamura T. Overexpression of lectin-like oxidized low-density lipoprotein receptor-1 induces intramyocardial vasculopathy in apolipoprotein E-null mice. *Circ Res* 2005;**97**:176–184.
15. Kuhlmann CR, Schäfer M, Li F, Sawamura T, Tillmanns H, Waldecker B *et al.* Modulation of endothelial Ca^{2+}-activated K^+ channels by oxidized LDL and its contribution to endothelial proliferation. *Cardiovasc Res* 2003;**60**:626–634.
16. Busse R, Fleming I. Vascular endothelium and blood flow. *Handb Exp Pharmacol* 2006;**176**:43–78.
17. Landmesser U, Drexler H. Endothelial function and hypertension. *Curr Opin Cardiol* 2007;**4**:316–320.
18. Brandes RP, Behra A, Lebherz C, Böger RH, Bode-Böger SM, Phivthong-Ngam L *et al.* N(G)-nitro-L-arginine- indomethacin-resistant endothelium-dependent relaxation in the rabbit renal artery: effect of hypercholesterolemia. *Atherosclerosis* 1997;**135**:49–55.
19. Honda H, Moroe H, Fujii H, Arai K, Notoya Y, Kogo H. Short term hypercholesterolemia alters N(G)-nitro-L-arginine and indomethacin-resistant endothelium relaxation by acetylcholine in rabbit renal artery. *Jpn J Pharmacol* 2001;**85**:203–206.
20. Köhler R, Hoyer J. The endothelium-derived hyperpolarizing factor: insights from genetic animal models. *Kidney Int* 2007;**72**:145–150.
21. Félétou M, Vanhoutte PM. Endothelium-derived hyperpolarizing factor: where are we now? *Arterioscler Thromb Vasc Biol* 2006;**26**:1215–1225.
22. Michaelis UR, Fleming I. From endothelium-derived hyperpolarizing factor (EDHF) to angiogenesis: Epoxyeicosatrienoic acids (EETs) and cell signaling. *Pharmacol Ther* 2006;**111**:584–595.
23. Tanaka Y, Koike K, Toro L. MaxiK channels roles in blood vessel relaxation induced by endothelium-derived relaxing factors and their molecular mechanisms. *J Smooth Muscle Res* 2004;**40**:125–153.
24. Münzel T, Afanas'ev IB, Kleschyov AL, Harrison DG. Detection of superoxide in vascular tissue. *Arterioscler Thromb Vasc Biol* 2002;**22**:1761–1768.
25. Bolann BJ, Ulvik RJ. Release of iron from ferritin by xanthine oxidase. Role of the superoxide radical. *Biochem J* 1987;**243**:55–59.

26. Neidhold S, Eichhorn B, Kasper M, Ravens U, Kaumann AJ. The function of alpha- and beta-adrenoceptors of the saphenous artery in caveolin-1 knockout and wild-type mice. *Br J Pharmacol* 2007;**150**:261–270.
27. Wuest M, Eichhorn B, Braeter M, Strugala G, Michel MC, Ravens U. Muscarinic receptor expression and receptor-mediated detrusor contraction: comparison of juvenile and adult porcine tissue. *Pflugers Arch* 2008; **456**:349–358.
28. Jiang B, Wu L, Wang R. Sulphonylureas induced vasorelaxation of mouse arteries. *Eur J Pharmacol* 2007;**577**:124–128.
29. Matsumoto T, Kakami M, Kobayashi T, Kamata K. Gender differences in vascular reactivity to endothelin-1 (1–31) in mesenteric arteries from diabetic mice. *Peptides* 2008;**29**:1338–1346.
30. Busse R, Edwards G, Félétou M, Fleming I, Vanhoutte PM, Weston AH. EDHF: bringing the concepts together. *Trends Pharmacol Sci* 2002;**23**: 374–380.
31. Campbell WB, Falck JR. Arachidonic acid metabolites as endothelium-derived hyperpolarizing factors. *Hypertension* 2007;**49**:590–596.
32. Shimokawa H, Matoba T. Hydrogen peroxide as an endothelium-derived hyperpolarizing factor. *Pharmacol Res* 2004;**49**:543–549.
33. Li HF, Chen SA, Wu SN. Evidence for the stimulatory effect of resveratrol on Ca^{2+}-activated K^+ current in vascular endothelial cells. *Cardiovasc Res* 2000;**4**:1035–1045.
34. Bentzen BH, Nardi A, Calloe K, Madsen LS, Olesen SP, Grunnet M. The small molecule NS11021 is a potent and specific activator of Ca^{2+}-activated big-conductance K^+channels. *Mol Pharmacol* 2007;**72**: 1033–1044.
35. Libinaki R, Heffernan M, Jiang WJ, Ogru E, Ignjatovic V, Gianello R *et al.* Effects of genetic and diet-induced obesity on lipid metabolism. *IUBMB Life* 1999;**48**:109–113.
36. Gallou-Kabani C, Vigé A, Gross MS, Rabès JP, Boileau C, Larue-Achagiotis C *et al.* C57BL/6J and A/J mice fed a high-fat diet delineate components of metabolic syndrome. *Obesity* 2007;**15**:1996–2005.
37. Cannon CP. High-density lipoprotein cholesterol and residual cardiometabolic risk in metabolic syndrome. *Clin Cornerstone* 2007;**8**:14–12.
38. Xie H, Bevan JA. Oxidized low-density lipoprotein enhances myogenic tone in the rabbit posterior cerebral artery through the release of endothelin-1. *Stroke* 1999;**30**:2423–2429.
39. Galle J, Mameghani A, Bolz SS, Gambaryan S, Görg M, Quaschning T *et al.* Oxidized LDL and its compound lysophosphatidylcholine potentiate AngII-induced vasoconstriction by stimulation of RhoA. *J Am Soc Nephrol* 2003;**14**:1471–1479.
40. Ge ZD, Zhang XH, Fung PC, He GW. Endothelium-dependent hyperpolarization and relaxation resistance to N(G)-nitro-L-arginine and indomethacin in coronary circulation. *Cardiovasc Res* 2000;**46**:547–556.
41. Huang A, Sun D, Smith CJ, Connetta JA, Shesely EG, Koller A *et al.* In eNOS knockout mice skeletal muscle arteriolar dilation to acetylcholine is mediated by EDHF. *Am J Physiol Heart Circ Physiol* 2000;**278**:762–768.
42. Freiman PC, Mitchell GG, Heistad DD, Armstrong ML, Harrison DG. Atherosclerosis impairs endothelium-dependent vascular relaxation to acetylcholine and thrombin in primates. *Circ Res* 1986;**58**:783–789.
43. Kugiyama K, Kerns SA, Morrisett JD, Roberts R, Henry PD. Impairment of endothelium-dependent arterial relaxation by lysolecithin in modified low-density lipoproteins. *Nature* 1990;**344**:160–162.
44. Golino P, Piscione F, Willerson JT, Cappelli-Bigazzi M, Focaccio A, Villari B *et al.* Divergent effects of serotonin on coronary-artery dimensions and blood flow in patients with coronary atherosclerosis and control patients. *N Engl J Med* 1991;**324**:641–648.
45. Saran M, Michel C, Bors W. Reaction of NO with O^{2-} implications for the action of endothelium-derived relaxing factor (EDRF). *Free Radic Res Commun* 1990;**10**:221–226.
46. Huie RE, Padmaja S. The reaction of no with superoxide. *Free Radic Res Commun* 1993;**18**:195–199.
47. Rueckschloss U, Galle J, Holtz J, Zerkowski HR, Morawietz H. Induction of NAD(P)H-oxidases by oxidized low-density lipoprotein in human endothelial cells: antioxidative potential of hydroxymethylglutaryl coenzyme A reductase inhibitor therapy. *Circulation* 2001;**104**:1767–1772.
48. Stielow C, Catar RA, Muller G, Wingler K, Scheurer P, Schmidt HH *et al.* Novel Nox inhibitor of oxLDL-induced reactive oxygen species formation in human endothelial cells. *Biochem Biophys Res Commun* 2006;**344**: 200–205.
49. Lehoux S. Redox signalling in vascular responses to shear and stretch. *Cardiovasc Res* 2006;**71**:269–279.
50. Wareing M, Bai X, Seghier F, Turner CM, Greenwood SL, Baker PN *et al.* Expression and function of potassium channels in the human placental vasculature. *Am J Physiol Regul Integr Comp Physiol* 2006;**291**:437–446.
51. Sandow SL, Tare M, Coleman HA, Hill CE, Parkington HC. Involvement of myoendothelial gap junctions in the action of endothelium-derived hyperpolarizing factor. *Circ Res* 2002;**90**:1108–1113.
52. Dora KA, Sandow SL, Gallagher NT, Takano H, Rummery NM, Hill C *et al.* Myoendothelial gap junctions may provide the pathway for EDHF in mouse mesenteric artery. *J Vasc Res* 2003;**40**:480–490.
53. Haddy FJ, Vanhoutte PM, Félétou M. Role of potassium in regulating blood flow and blood pressure. *Am J Physiol* 2005;**290**:R546–R552.
54. Prior HM, Webster N, Quinn K, Beech DJ, Yates MS. K^+-induced dilation of a small renal artery: no role for inward rectifier K^+ channels. *Cardiovasc Res* 1998;**37**:780–790.
55. Nelson MT, Quayle JM. Physiological roles and properties of potassium channels in arterial smooth muscle. *Am J Physiol* 1995;**268**:799–822.
56. Larsen BT, Gutterman DD, Sato A, Toyama K, Campbell WB, Zeldin DC *et al.* Hydrogen peroxide inhibits cytochrome P450 epoxygenases: interaction between two endothelium-derived hyperpolarizing factors. *Circ Res* 2008;**102**:59–67.
57. Yang Q, Yima AP, He GW. The significance of endothelium-derived hyperpolarizing factor in the human circulation. *Curr Vasc Pharmacol* 2007;**5**: 85–92.
58. Spector AA, Norris AW. Action of epoxyeicosatrienoic acids on cellular function. *Am J Cell Physiol* 2007;**292**:996–1012.
59. Archer SL, Gragasin FS, Wu X, Wang S, McMurtry S, Kim DH *et al.* Endothelium-derived hyperpolarizing factor in human internal mammary artery is 11,12-epoxyeicosatrienoic acid and causes relaxation by activating smooth muscle BK(Ca) channels. *Circulation* 2003;**107**: 769–776.
60. Urakami-Harasawa L, Shimokawa H, Nakashima M, Egashira K, Takeshita A. Importance of endothelium-derived hyperpolarizing factor in human arteries. *J Clin Invest* 1997;**100**:2793–2799.
61. Eichhorn B, Dobrev D. Vascular large conductance calcium-activated potassium channels: Functional role and therapeutic potential. *Naunyn Schmiedebergs Arch Pharmacol* 2007;**376**:145–155.
62. Ambroisine ML, Favre J, Oliviero P, Rodriguez C, Gao J, Thuillez C *et al.* Aldosterone-induced coronary dysfunction in transgenic mice involves the calcium-activated potassium (BK_{Ca}) channels of vascular smooth muscle cells. *Circulation* 2007;**116**:2435–2443.

[mAbs 1:4, 1-7; July/August 2009]; ©2009 Landes Bioscience

Report

Generation and characterization of chicken monoclonal antibodies against human LOX-1

Shin Iwamoto,[1] Norihisa Nishimichi,[1] Yoshiko Tateishi,[1] Yuko Sato,[2] Hiroyuki Horiuchi,[1] Shuichi Furusawa,[1] Tatsuya Sawamura[2] and Haruo Matsuda[1,*]

[1]Laboratory of Immunobiology; Department of Molecular and Applied Bioscience; Graduate School of Biosphere Science; Hiroshima University; Higashi-Hiroshima, Hiroshima Japan; [2]Department of Vascular Physiology; National Cardiovascular Center Research Institute; Suita, Osaka Japan

Abbreviations: LOX-1, lectin-like oxidized low-density lipoprotein receptor-1; LDL, low-density lipoprotein; oxLDL, oxidized low-density lipoprotein; CTL, C-type lectin-like; DNP, 2,4-dinitrophenyl

Key words: LOX-1, oxLDL, chicken monoclonal antibody, chimeric antibody, neutralizing antibody

Lectin-like oxidized low-density lipoprotein (LDL) receptor-1 (LOX-1) is the major receptor for oxidized LDL (oxLDL), and plays a key role in the pathogenesis of atherosclerosis and cardiovascular diseases. Monoclonal antibodies (mAbs) specific for human LOX-1 (hLOX-1) were generated by a phage display technique using chickens immunized with recombinant hLOX-1 (rhLOX-1). A total of 53 independent scFv clones reactive for rhLOX-1 were obtained. Of the 53 clones, 49 recognized the C-type lectin-like domain (CTL domain), which contributes to the binding of oxLDL. Of these, 45 clones inhibited oxLDL-binding with LOX-1. Furthermore, some of these clones cross-reacted with rabbit, pig and/or mouse LOX-1. For possible application as therapeutic agents in the future, two cross-reactive mAbs were re-constructed as chicken-human chimeric antibodies. The chimeric antibodies showed similar characteristics compared to the original antibodies, and inhibited oxLDL binding to LOX-1 expressed on CHO cells. The results obtained in this study indicate that anti-LOX-1 mAbs might be useful tools for functional analyses and development of therapeutic agents for cardiovascular indications such as atherosclerosis.

Introduction

LOX-1 was first identified in vascular endothelial cells, and has been characterized as the major receptor for oxLDL in endothelial cells.[1] Studies have indicated that LOX-1 has a critical role in the pathogenesis of atherosclerosis and cardiovascular diseases.[2] Recently, a soluble form of LOX-1 (sLOX-1) released by proteolytic cleavage was detected in serum from acute coronary syndrome (ACS) patients.[3] This suggests that sLOX-1 might be a useful biomarker for early diagnosis of ACS.

LOX-1 is a 50 kDa type-II membrane protein that, as assessed by structure, belongs to the C-type lectin family. LOX-1 consists of four domains, the N-terminal intracellular domain, the transmembrane domain, the Neck domain, and the CTL domain.[4] Among these, the CTL domain is critical for LOX-1 function, as the C-terminal residues and arginine residues in this domain are essential for oxLDL-binding.[5-7]

Although mAbs specific to LOX-1 are useful for expression and functional analyses of LOX-1,[1,5,8-11] the number of anti-LOX-1 mAbs is insufficient[1,5,9,11] at least in part because generation of mAbs against LOX-1 by immunization of mammalian species is difficult due to the high conservation of the CTL domain among mammals.[5]

However, the chicken is a useful animal for developing specific antibodies against conserved mammalian proteins because of the phylogenic differences between chickens and mammals.[12-15] In fact, numerous chicken mAbs have been produced using cell fusion and phage-display techniques.[12-15] Although a LOX-1 homolog has not yet been found in chickens, useful mAbs against mammalian LOX-1 can be produced by immunizing chickens. To study chicken mAbs against various LOX-1 epitopes, we generated 53 chicken mAbs specific to LOX-1 by a phage-display technique using chickens immunized with rhLOX-1. Here, we report data for 49 mAbs that recognized the CTL domain, of which 45 also inhibited oxLDL-binding with LOX-1.

Results

Production of recombinant LOX-1. Recombinant human, mouse, rabbit and pig versions of LOX (rhLOX-1, rmLOX-1, rrLOX-1 and rpLOX-1) as well as delta Neck, were each produced in FreeStyle™ 293-F cells. These recombinant LOX-1 proteins were detected as approximately 62 kDa, 40 kDa, 20 kDa, 22 kDa and 30 kDa bands, respectively, on SDS-PAGE under non-reducing conditions (Fig. 1A). rhLOX-1 and delta Neck were each detectable

*Correspondence to: Haruo Matsuda; Laboratory of Immunobiology; Department of Molecular and Applied Bioscience; Graduate School of Biosphere Science; 1-4-4 Kagamiyama; Higashi-Hiroshima; Hiroshima 739-8528 Japan; Fax: +81.82.424.7968; Email: hmatsu@hiroshima-u.ac.jp

Submitted: 09/04/08; Accepted: 05/04/09

Previously published online as a *mAbs* E-publication:
http://www.landesbioscience.com/journals/mabs/article/8919

as a half-molecule bands under reducing conditions (data not shown). These results confirmed that rhLOX-1 and delta Neck are cross-linked by a disulfide bond through Cys140.[7] The proteins exhibited binding activity toward human oxLDL, but not the negative control LDL (Fig. 1B). The result suggests that the recombinant proteins maintained the correct structure and function. rmLOX-1, rrLOX-1 and rpLOX-1 were monomers; these proteins showed the same profiles under both reducing and non-reducing conditions. Recombinant LOX-1s (human, mouse, rabbit and pig) were detected as broad bands or two bands (Fig. 1A). LOX-1s contains putative N-glycosylation signals,[5] so the differences in molecular weight (MW) between these bands are probably due to variation in glycosylation.

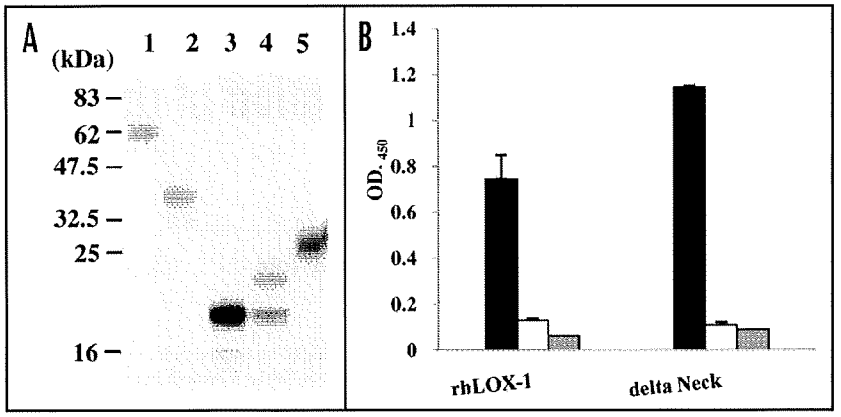

Figure 1. SDS-PAGE profiles and reactivity of recombinant LOX-1s. (A) SDS-PAGE profiles of rhLOX-1 (lane 1), delta Neck (lane 2), rmLOX-1 (lane 3), rrLOX-1 (lane 4) and rpLOX-1 (lane 5). Recombinant proteins were purified from the supernatant of 293-F cells by nickel affinity chromatography. All samples were subjected to SDS-PAGE under non-reducing conditions and were stained with CBBR. Numbers on the right indicate apparent molecular masses in kDa. (B) Reactivity of rhLOX-1 and delta Neck to oxLDL (black), LDL (negative control, white) and BSA (control, gray) was measured by ELISA using biotin-labeled rhLOX-1- or delta Neck-coated plates. Data are means ± SD of three independent experiments.

Specific antibodies against LOX-1. By using spleen cells from chickens immunized with rhLOX-1, the scFv phage library (5.0×10^8 cfu) was constructed. After the 6th round of panning selection against rhLOX-1, the specificity of the concentrated scFv phage library was examined by ELISA. Of 207 scFv phage clones from libraries of the 5th and 6th pannings, 113 were reactive for rhLOX-1 (data not shown). The results of nucleic acid sequencing in the positive clones showed that these clones could be subclassified to 51 independent clones (data not shown). In the panning selections against rmLOX-1 using the same phage-display library, 2 independent clones were selected from libraries of the 3rd and 4th pannings. Finally, a total of 53 clones were constructed as rIgY for quantitative experiments.

Reactivity of recombinant antibodies against LOX-1s. We investigated whether 53 chicken antibodies obtained by phage-display technique recognize the CTL or Neck domains and LOX-1 from other mammalian species.

The reactivities of the 53 rIgY antibodies against LOX-1 were assessed by ELISA and FACS. Of 53 clones, HUC5-34, HUC5-40, HUC6-34 and HUC6-41, reacted with rhLOX-1, but not with delta Neck (Fig. 2A). The result suggests that these four clones recognize the Neck domain of LOX-1 (anti-Neck domain clones). The residual clones reacted with both rhLOX-1 and delta Neck with similar intensities (data not shown), indicating that they recognize the CTL domain.

Seven (HUC52, HUC5-44, HUC5-53, HUC5-63, HUC5-90, HUC6-92 and HUC3-48) of 53 clones were cross-reactive with both rabbit and pig LOX-1 (Fig. 2B). HUC5-24 cross-reacted with rrLOX-1 (Fig. 2B), and HUC5-9 reacted with rpLOX-1 (Fig. 2B). The two clones (HUC3-1 and HUC3-48) selected from panning against rmLOX-1 were reactive with rmLOX-1. Interestingly, HUC3-48 reacted with LOX-1s from all species tested (Fig. 2B). However, in western blotting these clones did not react with recombinant LOX-1s (data not shown), indicating that these clones recognize conformational epitopes. In fact, these clones also reacted with LOX-1-expressing cells in FACS analysis (data not shown). None of the clones tested reacted with BSA and wild type CHO cells (data not shown).

Neutralization activity of anti-LOX-1 antibodies. LOX-1 is expressed in atherosclerosis and several cardiovascular diseases, such as myocardial ischemia.[2] In a rat model, administration of anti-LOX-1 antibody effectively suppressed intimal hyperplasia.[10] Thus, inhibition of LOX-1 activity may be a useful strategy to produce novel drugs for cardiovascular disorders. The neutralization activity of 53 anti-LOX-1 antibodies was examined using a modified method described previously.[19] Forty-five of 53 clones showed neutralization activity (data not shown), suggesting that these clones recognized the CTL domain, which is essential for oxLDL-binding.[5] Although the Neck domain of LOX-1 is not critical for oxLDL binding with LOX-1, anti-Neck domain clones HUC5-34, HUC5-40, HUC6-34 and HUC6-41 (Fig. 2A) slightly inhibited oxLDL-binding (data not shown). The MW of rhLOX-1 is about 62 kDa (Fig. 1A, lane 1), and that of rIgY is about 250 kDa.[17] With MW four-fold greater than rhLOX-1, anti-Neck domain clones likely exhibited steric inhibition.

To have potential as therapeutic agents, two clones, HUC52, which cross-reacted with rabbit and pig LOX-1, and HUC3-48, which recognized LOX-1s from all species tested, were re-constructed as chimeric IgG antibodies (Fig. 3). In order to avoid Ig effector functions involving complement activation and antibody-dependent cell-mediated cytotoxicity, the IgG4 subclass was selected. The chimeric antibodies had similar reaction patterns compared to their original rIgY forms (Fig. 4). Inhibition studies were then performed using LOX-1-expressing CHO cells. Regardless of the animal species tested, the two chimeric IgGs reacted with LOX-1-expressing CHO cells (Fig. 5A), and blocked oxLDL-binding to LOX-1-expressing CHO cells (Fig. 5B). HUC3-48 also showed inhibition activity against mouse LOX-1-expressing cells (data not shown).

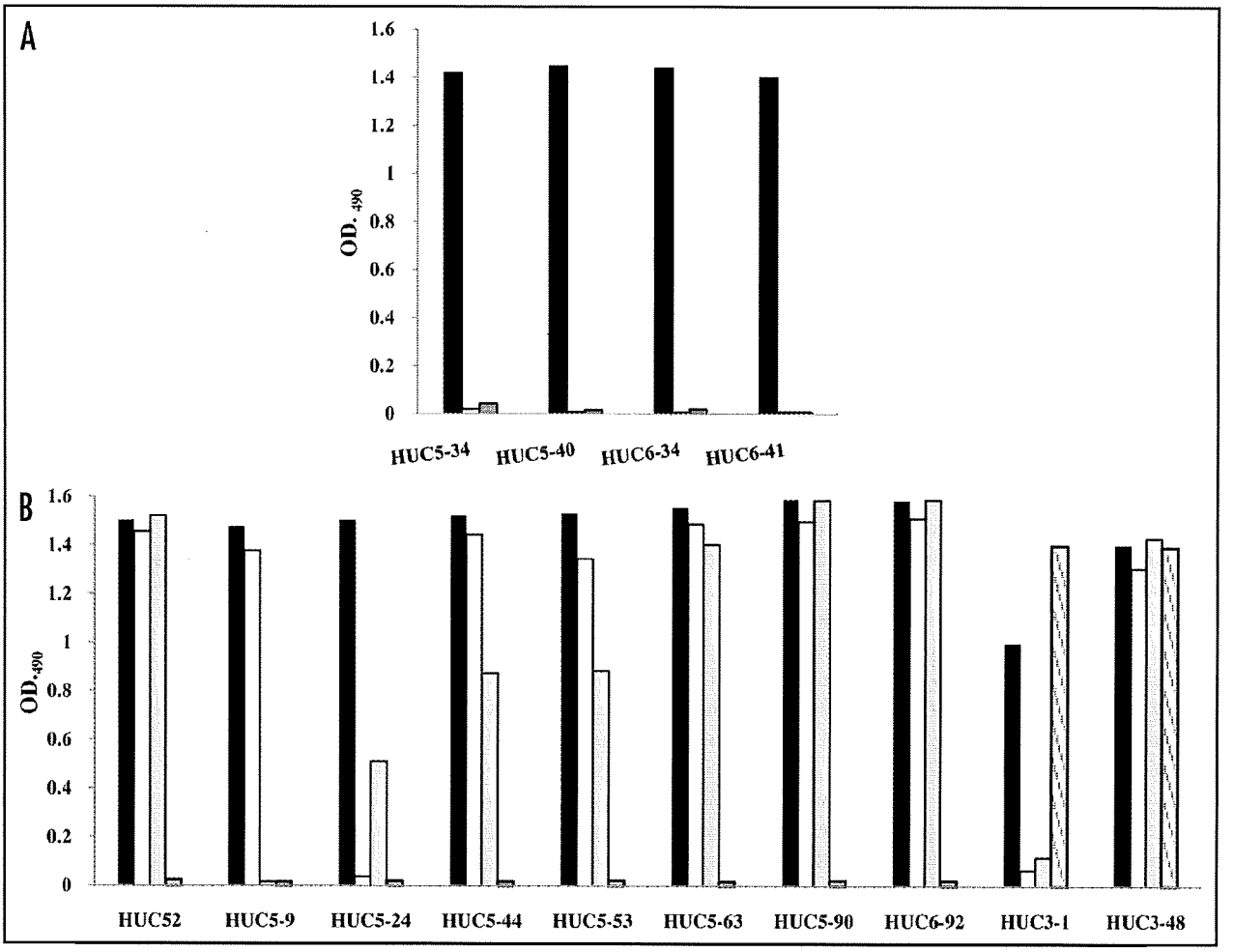

Figure 2. Reactivity of rIgY antibodies against recombinant LOX-1s. (A) Reactivity of rIgY antibodies against rhLOX-1 and delta NECK. rIgYs (1 μg/ml) were added to wells coated with biotinylated rhLOX-1 (black), delta Neck (white) or BSA (negative control, gray). (B) Cross-reactivity of 53 rIgY antibodies against LOX-1 from four species. The rIgYs (1 μg/ml) were added wells coated with biotinylated rhLOX-1 (black), rpLOX-1 (white), rrLOX-1 (gray) or rmLOX-1 (shaded). Of the 53 clones, eight cross-reacted with rrLOX-1 and/or rpLOX-1 and only two clones also recognized rmLOX-1.

Discussion

LOX-1 is the main receptor for oxLDL on endothelial cells, and it mediates the recognition and internalization of oxLDL.[1] Recent studies on LOX-1 have shown that this molecule plays a critical role in the development of atherosclerosis and cardiovascular diseases.[2] For further research into the function of LOX-1, LOX-1-specific mAbs are thought to be one of the most useful tools for basic analysis and clinical applications. However, a limited number of mAbs against human LOX-1 have been reported. This might be because the CTL domain is highly conserved among mammalian species[5] and so anti-LOX1 mAbs are difficult to generate. We have successfully produced chicken mAbs against conserved mammalian molecules using cell fusion and phage-display techniques.[12-15] In the present study, a total of 53 scFv chicken mAbs specific for LOX-1 were generated from only two panning selections. Most of the rIgY forms from these scFv antibodies recognized the CTL domain of LOX-1, and only 4 clones recognized the Neck domain (Fig. 2A). These results indicate that the chicken is a useful animal for producing antibodies specific for mammalian LOX-1, particularly the CTL domain.

Mice, rabbits and pig are typically used as models for atherosclerosis and cardiovascular diseases. For example, ApoE-knockout mice and Watanabe heritable hyperlipidemic rabbits are used as animal models of spontaneous hyperlipidemia and in the analysis of LOX-1 function.[16,18-21] Therefore, we investigated whether the mAbs presented here cross-react with LOX-1s from these model animals. Six clones (HUC52, HUC5-44, HUC5-53, HUC5-63, HUC5-90 and HUC6-92) that reacted with rhLOX-1 also displayed cross-reactivity to both rrLOX-1 and rpLOX-1 (Fig. 2B). In contrast, no rmLOX-1 cross-reactive antibodies were obtained in the first antibody selection. We then selected antibodies using the scFv phage library from rhLOX-1-immunized chickens, and identified clones HUC3-1, which cross-reacted with rmLOX-1 and rhLOX-1, and HUC3-48, which cross-reacted with recombinant LOX-1s from all three species examined (Fig. 2B).

A total of 45 rIgYs including HUC3-48 mAb inhibited oxLDL-binding with LOX-1 (data not shown). The result indicates that these 45 mAbs are reactive for the CTL domain, which is critical for the binding of oxLDL.[5]

For possible utilization as therapeutic antibody agents for humans, we reconstructed two clones as chicken-human chimeric IgG by converting the chicken constant regions into human regions (Fig. 3). These antibodies were evaluated in inhibition assays using cells expressing LOX-1. HUC52 and HUC3-48 chimeric IgGs, which had similar LOX-1 reactivity compared to their respective parental antibodies (Fig. 4), blocked oxLDL binding to LOX-1 expressed on CHO cells (Fig. 5B). This evidence suggests that these antibodies should be further evaluated in animal models.

Since the variability of FR residues in chicken antibodies is very small compared to those in human and rodent, it is possible that the same human template can be used to humanize all chicken antibodies. Humanization of chicken mAbs has been achieved by CDR-grafting, followed by framework fine-tuning using a phage displayed combinatorial library.[22] In the current study, chicken mAbs were successfully humanized as divalent IgG4 without loss of antibody affinity. Therefore, humanized chicken antibodies may have applications as treatments for human disease in the future.

In conclusion, we generated 53 mAbs against LOX-1 using phage-display techniques and 45 of these mAbs that recognized the CTL domain were neutralizing antibodies. In addition, two human chimeric mAbs from HUC52 and HUC3-48, cross-reacted with rabbit, pig or mouse LOX-1, also showed neutralization activitities against LOX-1 expressing cells. These results indicate that our mAb clones might be useful tools for the investigation of LOX-1 function, and might have clinical applications. Production of chicken-mouse, chicken-rabbit and chicken-pig chimeric mAbs for preclinical studies using animal models is in progress.

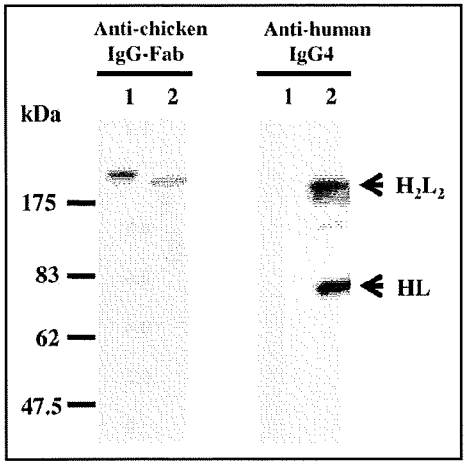

Figure 3. Western blot analysis of recombinant chicken antibody and chicken-human chimeric antibody. The rIgY (lane 1) and chimeric IgG (lane 2) were each run on 10% SDS-polyacrylamide gels under non-reducing conditions. Anti-chicken IgG-Fab and anti-human IgG4 were used as a detection antibody. Numbers on the right indicate apparent molecular masses in kDa. H_2L_2 represents antibody full length and HL indicates the halved molecule.

Materials and Methods

Antigens. Recombinant human LOX-1 (amino acids 61–273; rhLOX-1) and its deletion mutant (amino acids 137–273; delta Neck), recombinant mouse LOX-1 (amino acids 188–363 of mouse LOX-1; rmLOX-1), recombinant rabbit LOX-1 (amino acids 101–278 of rabbit LOX-1; rrLOX-1) and recombinant pig LOX-1 (amino acids 61–274 of pig LOX-1; rpLOX-1) were generated with pcDNA4/myc-HisA (Invitrogen, USA) in order to synthesize each LOX-1 as a 6xHistidine tag (His tag) fusion protein as described previously.[18] Proteins were produced in a FreeStyle™ 293 Expression System (Invitrogen) and were purified using a Probond protein purification kit (Invitrogen), and their molecular sizes were confirmed by SDS-PAGE. Purified proteins were also biotinylated using a Biotin Labeling Kit-NH_2 (Dojindo, Japan). The PCR primers used in this study were shown in Table 1.

Cells. cDNA encoding the human LOX-1 was subcloned into a Tet-On Gene Expression vector pTRE2 hyg (Clontech Laboratories, USA). The plasmid was transfected into CHO-K1 Tet-On cells

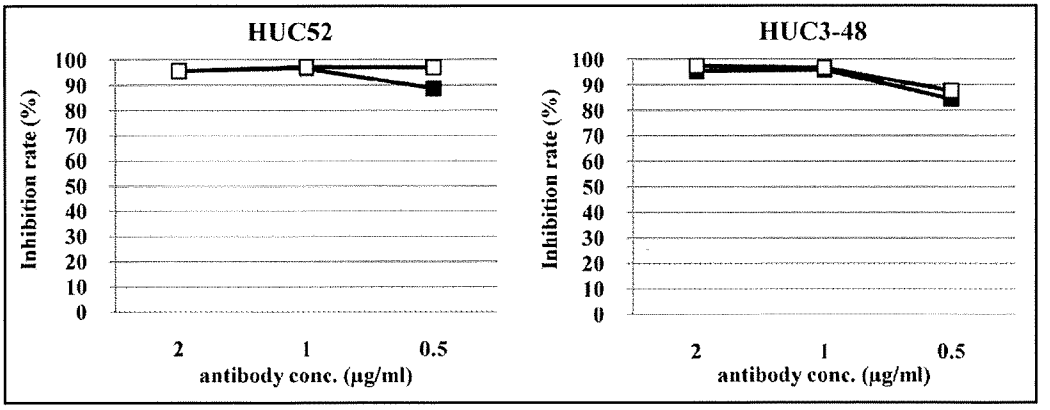

Figure 4. Inhibition of oxLDL-binding with LOX-1 by anti-LOX-1 antibodies. rhLOX-1 was used as the capture molecule. rIgY (closed square) or chimeric IgG (open square) indicated inhibition rate of oxLDL-binding with LOX-1 using anti-human ApoB antibody. Anti-DNP rIgY was used as a negative control and standard for comparison.

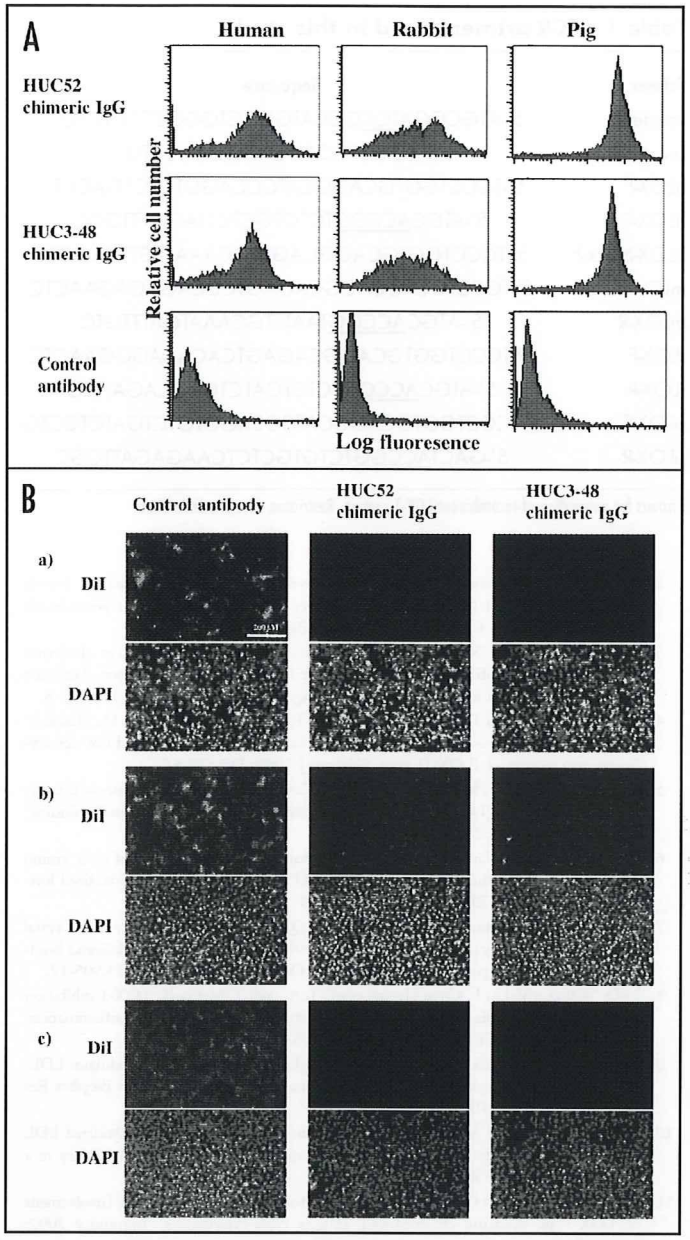

Figure 5. Reactivities and blocking activities of chimeric IgGs against LOX-1-expressing cells. (A) LOX-1-expressing CHO cells were incubated with chimeric IgG (1 μg/ml) revealed with FITC-labeled anti-human IgG. Fluorescence was analyzed by FACS. (B) Human (a), rabbit (b) or pig (c) LOX-1-expressing CHO cells were incubated with chimeric IgG (5 μg/ml). DiI-labeled oxLDL (3 μg/ml) was added for 2 h. After that, the cells were fixed with 4% (v/v) paraformaldehyde. Then, the nuclei of the cells was counterstained with DAPI and subjected to observation with fluorescence microscopy.

(Clontech Laboratories) by Lipofectamin2000 tansfection reagent (Invitrogen) according to the manufacture's instruction. Stably transformants were selected under Ham's F12/10% fetal bovine serum (FBS) supplemented with 400 μg/ml hygromycin B (Wako, Japan). The cells expressing LOX-1 in response to doxycycline (Wako) were selected. The LOX-1 expression was induced with 1 μg/ml doxycyline for 24 h before the experiments. Rabbit and pig cDNA were subcloned into a mammalian expression vector *p*EF6V5-HisA (Invitrogen), respectively. The plasmid was each transfected into CHO-K1 cells by FuGENE HD transfect reagent (Roche Diagnostics, Switzerland). Stably LOX-1-expressing cells were selected and maintained under Ham's F12/10% FBS supplemented with 8 μg/ml blasticidin S (Invitrogen).

Immunization and construction of phage-display library. Chicken scFv mAbs were generated by the chicken phage-display technique.[15] One-month-old H-B15 inbred chickens were immunized intraperitoneally (i.p.) with rhLOX-1 (50 μg/ml/chicken) in an equal volume of alum solution (ALUM). The chickens received three additional i.p. injections with the same antigen together with ALUM at 3-week intervals. Four days after the final injection, spleen cells were isolated from immunized chickens. RNA was extracted from spleen cells, immunoglobulin variable region (VH and VL) genes were amplified and a scFv phage library was constructed as described previously.[15]

Panning selection. The phage-display scFv library from rhLOX-1-immunized chickens was panned against rhLOX-1 or rmLOX-1. For selection of rhLOX-1-specific antibodies, 100 μl (10 μg/ml) of rhLOX-1 was coated on a Maxisorp Nunc-Immuno™ module (NUNC, USA). An ELISA plate was then blocked with 2% (w/v) non-fat dried milk powder (EuroClon, Italia) in phosphate-buffered saline (PBS) at room temperature (RT) for 1 h. For selection against rmLOX-1, 100 μl (5 μg/ml) of biotin-labeled rmLOX-1 was coated on Nunc Immobilizer™ Streptavidin plates (NUNC). Panning selection was performed as described previously.[15]

Recombinant chicken IgY (rIgY) and chicken-human chimeric IgG4 antibody (chimeric IgG). The rIgY and chimeric IgG were generated using the VH and VL genes from phage-displayed chicken antibodies obtained in this study, and plasmid vectors[17,23] were used for construction of the light and heavy chains, respectively. Constructed plasmid DNAs were transfected into COS-7 cells or FreeStyle™ 293-F cells (Invitrogen) using FuGENE HD transfect reagent.

Western blotting. Western blotting for detection of recombinant LOX-1s was carried out. Recombinant LOX-1s were subjected to SDS-PAGE under non-reducing conditions, and were then transferred to an Immun-Blot™ PVDF membrane (Bio-Rad, USA) at 350 mA for 1 h. Membranes were incubated for 1 h at room temperature with chicken anti-LOX-1 rIgYs and developed by ECL plus (GE Healthcare, UK). Chemiluminescent signals were then analyzed using a LAS-3000 (Fuji Film, Japan).

Western blotting for detection of rIgY and chimeric IgG was carried out as described previously.[17,18] Horseradish peroxidase (HRP)-labeled anti-chicken IgG-Fab fragment (Bethyl, USA) was used for detection of rIgY and chimeric IgG. Mouse anti-human IgG4 antibody (BD Biosciences, USA) was used as the first antibody and HRP-labeled-mouse IgG antibody (Southern Biotech, USA) was used as the second antibody for detection of chimeric IgG. The rIgY and chimeric IgG were detected using ECL plus and LAS-3000.

ELISA for reactivity and cross-reactivity of rIgYs. The wells of Nunc Immobilizer™ Streptavidin plates were coated with 50

μl (1 μg/ml) of biotin-labeled rhLOX-1, delta Neck, rmLOX-1, rrLOX-1, rpLOX-1 or BSA (control antigen) in carbonate buffer (pH 9.5) for 1 h at RT. After washing with PBS-T, the respective rIgYs were added at 1 μg/ml. Plates were incubated at 37°C for 1 h. After washing with PBS-T, bound antibodies were detected using a HRP-labeled goat anti-chicken IgG (H + L) (Kirkeggaard and Perry Laboratories, USA). After washing with PBS-T, *o*-phenylene diamine sulfate (OPD, Sigma, USA) was added and the optical density was measured at 490 nm using a Model 680 microplate reader (Bio-Rad). Human anti-human LOX-1 mAb TS-92,[9] was used as a positive control.

FACS analysis. The recombinant antibodies were each incubated with LOX-1-expressing CHO cells at 4°C for 1 h in PBS containing 0.1% FBS and 0.1% NaN_3 (FACS buffer). After washing with FACS buffer, cells were incubated with FITC-labeled anti-chicken IgG (H + L) or anti-human IgG (H + L) (Southern Biotech, USA) for 30 min at 4°C. Fluorescence was analyzed by FACSCalibur (BD, USA).

Inhibition analysis by mAb in oxLDL-binding with recombinant LOX-1protein. Inhibition analysis was performed using a modified method reported previously.[16] Biotin-labeled rhLOX-1 (50 ng/well) was immobilized on Nunc Immobilizer™ Streptavidin plates by incubating at RT for 1 h in 50 μl of carbonate buffer. After washing with PBS, rIgY (1 μg/ml), TS-92 (positive control, 1 μg/ml) and anti-2,4-dinitrophenyl (DNP) rIgY (negative control, 1 μg/ml)[18] were each added to rhLOX-1-coated wells, and plates were incubated at RT for 2 h. After washing with PBS, plates were incubated overnight at 4°C with 50 μl of human oxLDL (3 μg/ml) in PBS containing 20% (vol/vol) newborn calf serum (NBCS, Gibco, USA). Plates were then washed with PBS, and incubated for 2 h at RT with the HRP-sheep anti-human ApoB polyclonal antibody (The Binding Site, UK) diluted 1,000 times with PBS containing 1% (w/v) BSA for detection of oxLDL. After washing with PBS, the peroxidase reaction was initiated by incubating plates for 5 min at RT with 50 μl of SureBlue Reserve™ TMB Microwell Peroxidase Substrate (Kirkegaard & Perry Laboratories, USA). The reaction was terminated with 0.1 M hydrochloric acid and 0.3 M sulfuric acid. Peroxidase activity was determined by measuring absorbance at 450 nm.

Inhibition analysis by mAb in oxLDL-binding with LOX-1expression cells. The LOX-1-expressing CHO cells were incubated with anti-LOX-1 antibody in Ham's F12 containing 10% NBCS for 1 h at 37°C. After 1 h, 1,1'-dioctadecyl-3,3,3',3'-tetramethylindocarbocyanine perchlorate (DiI, Molecular Probes, USA)-labeled oxLDL (3 μg/ml) was added to the cells for 2 h. The cells were washed three times with PBS and fixed with 4% (v/v) paraformaldehyde in PBS for 20 min. Then, the nuclei of the cells were counterstained with 5 μg/ml DAPI (Sigma) and subjected to observation with fluorescence microscopy.

Acknowledgements

This work was supported by the New Energy and Industrial Technology Development Organization (NEDO) of Japan.

Table 1 PCR primers used in this study

Primer	Sequence
Leader-F	5'-ATGCGGATCCGCCATGGCCTGGGCTCCTCTCCT
Leader-R	5'-TGCCTGCACCAGGGAACCTG
hLOX-F	5'-TCCCTGGTGCAGGCATCCCAGGTGTCTGACCTC
hLOX-R	5'-ATGCACCGGTCTGTGCTCTTAGGTTTGCC
hLOX-Neck-F	5'-TCCCTGGTGCAGGCAGTAGCAAATTGTTCAGCTC
mLOX-F	5'-TCCCTGGTGCAGGCAGAGTCCCAGAGAGAACTC
mLOX-R	5'-ATGCACCGGTAATTTGCAAATGATTTGTC
rLOX-F	5'-TCCCTGGTGCAGGCAGAGTCACAAAGGGAACTC
rLOX-R	5'-ATGCACCGGTCTCTGATCTCAGCAGATTTG
pLOX-F	5'-TCCCTGGTGCAGGCATCCCAGGTGTCTGATCTCCTG
pLOX-R	5'-GACTACCGGTCTGTGCTCTCAAGAGATTCGC

Primers for generation of recombinant LOX-1 protein. Restriction sites are underlined.

References

1. Sawamura T, Kume N, Aoyama T, Moriwaki H, Hoshikawa H, Aiba Y, et al. An endothelial receptor for oxidized low-density lipoprotein. Nature 1997; 386:73-7.
2. Mehta JL, Chen J, Hermonat PL, Romeo F, Novelli G. Lectin-like, oxidized low-density lipoprotein receptor-1 (LOX-1). A critical player in the development of atherosclerosis and related disorders. Cardiovasc Res 2006; 69:36-45.
3. Hayashida K, Kume N, Murase T, Minami M, Nakagawa D, Inada T, et al. Serum soluble lectin-like oxidized low-density lipoprotein receptor-1 levels are elevated in acute coronary syndrome: a novel marker for early diagnosis. Circulation 2005; 112:812-8.
4. Aoyama T, Sawamura T, Furutani Y, Matsuoka R, Yoshida MC, Fujiwara H, Masaki T. Structure and chromosomal assignment of the human lectin-like oxidized low-density-lipoprotein receptor-1 (LOX-1) gene. Biochem J 1999; 339:177-84.
5. Chen M, Narumiya S, Masaki T, Sawamura T. Conserved C-terminal residues within the lectin-like domain of LOX-1 are essential for oxidized low-density-lipoprotein binding. Biochem J 2001; 355:289-96.
6. Chen M, Inoue K, Narumiya S, Masaki T, Sawamura T. Requirements of basic amino acid residues within the lectin-like domain of LOX-1 for the binding of oxidized low-density lipoprotein. FEBS Lett 2001; 499:215-9.
7. Ohki I, Ishigaki T, Oyama T, Matsunaga S, Xie Q, Ohnishi-Kameyama M, et al. Crystal structure of human lectin-like, oxidized low-density lipoprotein receptor 1 ligand binding domain and its ligand recognition mode to OxLDL. Structure 2005; 13:905-17.
8. Li D, Williams V, Liu L, Chen H, Sawamura T, Antakli T, Mehta JL. LOX-1 inhibition in myocardial ischemia-reperfusion injury: modulation of MMP-1 and inflammation. Am J Physiol Heart Circ Physiol 2002; 283:1795-801.
9. Hu B, Li D, Sawamura T, Mehta JL. Oxidized LDL through LOX-1 modulates LDL-receptor expression in human coronary artery endothelial cells. Biochem Biophys Res Commun 2003; 307:1008-12.
10. Hinagata J, Kakutani M, Fujii T, Naruko T, Inoue N, Fujita Y, et al. Oxidized LDL receptor LOX-1 is involved in neointimal hyperplasia after balloon arterial injury in a rat model. Cardiovasc Res 2006; 69:263-71.
11. Delneste Y, Magistrelli G, Gauchat J, Haeuw J, Aubry J, Nakamura K, et al. Involvement of LOX-1 in dendritic cell-mediated antigen cross-presentation. Immunity 2002; 17:353-62.
12. Asaoka H, Nishinaka S, Wakamiya N, Matsuda H, Murata M. Two chicken monoclonal antibodies specific for heterophil Hanganutziu-Deicher antigen. Immunol Lett 1992; 32:91-6.
13. Matsushita K, Horiuchi H, Furusawa S, Horiuchi M, Shinagawa M, Matsuda H. Chicken monoclonal antibodies against synthetic bovine prion protein peptide. J Vet Med Sci 1998; 60:777-9.
14. Matsuda H, Mitsuda H, Nakamura N, Furusawa S, Mohri S, Kitamoto T. A chicken monoclonal antibody with specificity for the N-terminal of human prion protein. FEMS Immunol Med Microbiol 1999; 23:189-94.
15. Nakamura N, Shuyama A, Hojyo S, Shimokawa M, Miyamoto K, Kawashima T, et al. Establishment of chicken monoclonal antibody panel against prion protein. J Vet Med Sci 2004; 66:807-14.
16. Kakutani M, Ueda M, Naruko T, Masaki T, Sawamura T. Accumulation of LOX-1 ligand in plasma and atherosclerotic lesions of Watanabe heritable hyperlipidemic rabbits: identification by a novel enzyme immunoassay. Biochem Biophys Res Commun 2001; 282:180-5.
17. Shimamoto T, Nishibori N, Aosasa M, Horiuchi H, Furusawa S, Matsuda H. Stable production of recombinant chicken antibody in CHO-K1 cell line. Biologicals 2005; 33:169-74.

18. Sato Y, Nishimichi N, Nakano A, Takikawa K, Inoue N, Matsuda H, Sawamura T. Determination of LOX-1-ligand activity in mouse plasma with a chicken monoclonal antibody for ApoB. Atherosclerosis 2008; 200:303-9.
19. Inoue K, Arai Y, Kurihara H, Kita T, Sawamura T. Overexpression of lectin-like oxidized low-density lipoprotein receptor-1 induces intramyocardial vasculopathy in apolipoprotein E-null mice. Circ Res 2005; 97:176-84.
20. Xu X, Gao X, Potter BJ, Cao JM, Zhang C. Anti-LOX-1 rescues endothelial function in coronary arterioles in atherosclerotic ApoE knockout mice. Arterioscler Thromb Vasc Biol 2007; 27:871-7.
21. Chen M, Kakutani M, Minami M, Kataoka H, Kume N, Narumiya S, et al. Increased expression of lectin-like oxidized low density lipoprotein receptor-1 in initial atherosclerotic lesions of Watanabe heritable hyperlipidemic rabbits. Arterioscler Thromb Vasc Biol 2000; 20:1107-15.
22. Nishibori N, Horiuchi H, Furusawa S, Matsuda H. Humanization of chicken monoclonal antibody using phage-display system. Mol Immunol 2006; 43:634-42.
23. Nishibori N, Shimamoto T, Nakamura N, Shimokawa M, Horiuchi H, Furusawa S, Matsuda H. Expression vectors for chicken-human chimeric antibodies. Biologicals 2004; 32:213-8.

Suppression of Choroidal Neovascularization in Lectin-like Oxidized Low-Density Lipoprotein Receptor Type 1–Deficient Mice

Yasuya Inomata,[1] Mikiko Fukushima,[1] Ryuhei Hara,[1] Eri Takahashi,[1] Megumi Honjo,[2] Takahisa Koga,[1] Takahiro Kawaji,[1] Hiroo Satoh,[3] Motohiro Takeya,[3] Tatsuya Sawamura,[4] and Hidenobu Tanihara[1]

Purpose. To elucidate the role of the scavenger receptor, lectin-like oxidized low-density lipoprotein receptor type 1 (LOX-1), in the formation of choroidal neovascularization (CNV).

Methods. CNV was induced by laser photocoagulation of the ocular fundus in mice. The expression of LOX-1 mRNA and protein after laser injury was determined by real-time RT-PCR and Western blot analysis. Gelatin zymography was used to measure the activity of matrix metalloproteinase (MMP)-2 and pro-MMP-9, and ELISA was used to determine monocyte chemoattractant protein (MCP)-1 and vascular endothelial growth factor (VEGF) levels. At 14 days after laser injury, the extent of CNV was evaluated by fluorescein angiography and lectin staining using confocal microscopy.

Results. In wild-type mice, the relative expression level of LOX-1 mRNA compared with the control increased significantly 6 hours after laser injury and peaked 12 hours after laser injury ($P = 0.011$ and $P = 0.0006$, respectively), and the expression of LOX-1 protein was also detected 1 and 3 days after laser injury. Increases in MMP-2, pro-MMP2, and pro-MMP-9 after laser injury were reduced in LOX-1–deficient mice compared with wild-type mice. At 3 days after laser injury, increases in MCP-1 and VEGF significantly decreased in LOX-1–deficient mice compared with wild-type mice ($P = 0.014$ and $P = 0.001$, respectively). Morphometric analyses revealed that the induction of CNV formation was significantly inhibited in LOX-1–deficient mice.

Conclusions. These results suggest that LOX-1 plays an important role in the formation of CNV. This scavenging system might thus be a novel therapeutic target for CNV. (*Invest Ophthalmol Vis Sci.* 2009;50:3970–3976) DOI:10.1167/iovs.07-1177

Age-related macular degeneration (AMD) is the leading cause of legal blindness in persons older than 55 in developed countries.[1] Late AMD is subdivided into two forms, atrophic and (neovascular) exudative. The latter is associated with the most severe cases of visual loss caused by the growth of abnormal new vessels under the retinal pigment epithelium (RPE) from the choroid, leading to choroidal neovascularization (CNV). The pathogenesis of AMD is regarded as multifactorial, with age, genetic background, environmental risks, and systemic conditions playing important roles in its progression.[2–4] Although adhesion molecules, cytokines, and growth factors have been identified as contributing factors, the molecular mechanisms relating to AMD pathogenesis are not well understood.

Recently, similarities have been suggested between the pathogenesis of AMD and atherosclerosis.[5,6] During the progression of atherosclerosis, oxidized low-density lipoprotein (ox-LDL) and its specific receptors, so-called scavenger receptors (SRs), play a critical role in foam-cell formation after endothelial dysfunction and macrophage recruitment.[7] Interestingly, a previous clinical study identified elevated plasma levels of ox-LDL in patients with exudative AMD,[8] whereas the expression of ox-LDL SRs has been observed in surgically excised CNV.[8,9] Furthermore, several studies have shown that matrix metalloproteinases (MMPs) and chemokines, such as monocyte chemoattractant protein (MCP)-1, are involved in the remodeling and recruitment of leukocytes in atherosclerosis and CNV.[10–13]

Lectin-like ox-LDL receptor type 1 (LOX-1) is a recently identified SR expressed by vascular endothelial cells[14] that plays an important role in the formation of in vivo atherogenesis.[15] The induced expression of LOX-1 and its association with oxidative stress might also contribute to the formation of CNV in patients with AMD. Indeed, we previously demonstrated LOX-1 expression in surgically obtained CNV specimens from patients with AMD and other diseases.[16] Animal experiments have also revealed that LOX-1 is involved in inflammatory reactions of the eye through its regulation of leukocyte-endothelial interactions. Recent research into retinal angiogenic disorders has suggested that the inflammatory reaction is important in deterioration of the neovascular lesions, whereas the upregulated expression of LOX-1 in vascular endothelial cells has been shown to induce MMPs and MCP-1 expression.[17,18]

We hypothesized that elucidation of the potential roles and associated molecular mechanisms of LOX-1 could lead to the development of novel therapeutic modalities for AMD and other retinal angiogenic disorders. Here we report the upregulation of LOX-1 mRNA and protein expression in a mouse CNV model and suggest that LOX-1 and associated factors (such as

From the Departments of [1]Ophthalmology and Visual Science and [3]Cell Pathology, Kumamoto University Graduate School of Medical Sciences, Kumamoto, Japan; the [2]Department of Ophthalmology and Visual Science, Kyoto University Graduate School of Medicine, Kyoto, Japan; and the [4]Department of Vascular Physiology, National Cardiovascular Center, Osaka, Japan.

Supported in part by a Grant-in-Aid for Scientific Research from the Ministry of Education, Science, Sports and Culture, Japan, and the Ministry of Health and Welfare, Japan.

Submitted for publication September 9, 2007; revised February 25, July 9, November 22, and December 12, 2008; accepted May 27, 2009.

Disclosure: **Y. Inomata**, None; **M. Fukushima**, None; **R. Hara**, None; **E. Takahashi**, None; **M. Honjo**, None; **T. Koga**, None; **T. Kawaji**, None; **H. Satoh**, None; **M. Takeya**, None; **T. Sawamura**, None; **H. Tanihara**, None

The publication costs of this article were defrayed in part by page charge payment. This article must therefore be marked "*advertisement*" in accordance with 18 U.S.C. §1734 solely to indicate this fact.

Corresponding author: Yasuya Inomata, Department of Ophthalmology and Visual Science, Kumamoto University Graduate School of Medical Sciences, Honjo 1-1-1, Kumamoto 860-8556, Japan; inoyas@kxb.biglobe.ne.jp.

MMP-2, MMP-9, and MCP-1) contribute to the formation of CNV.

METHODS

Laser-Induced CNV in Mice

The generation and genotyping of LOX-1-deficient mice (on a C57BL/6 background) has been previously described.[15] The present study used 8-week-old C57BL/6 and LOX-1-deficient male mice. Laser-induced CNV was performed as described previously, with minor modifications.[19] Briefly, mice were anesthetized by intraperitoneal injection of 0.3 mL ketamine hydrochloride diluted (1:10) with sterile water. The pupils of the animals were dilated with 1% tropicamide, and krypton laser photocoagulation (spot size, 50 μm; duration, 0.05 second; power, 400 mW) burns were made to each retina using a slit lamp delivery system and a coverglass as a contact lens. For analysis of incident and extension of laser-induced CNV, CNV was induced in mice by three or four burns at the 6, 9, 12, and 3 o'clock positions around the optic disc. Any mouse with a hemorrhage or without an evident bubble (the sign of ruptured Bruch's membrane) was excluded from further analysis. The animals were maintained in a 12-hour light/12-hour dark cycle and had free access to food and water. All the mice were treated in accordance with the ARVO Statement for the Use of Animals in Ophthalmic and Vision Research.

Real-Time Reverse Transcription–Polymerase Chain Reaction

At 6 hours, 12 hours, 1 day, 2 days, 7 days, and 14 days after laser injury (10 burns), the eyes were dissected immediately, and total RNA was isolated from the posterior segment with an RNA isolation kit (AquaPure; Bio-Rad Laboratories, Hercules, CA). To remove genomic DNA, the total RNA preparation was treated with DNase-I (Invitrogen, Carlsbad, CA). Assay-on-demand primers and probes systems (Applied Biosystems, Foster City, CA) were used to quantify the mRNAs for a mouse LOX-1 assay (ID Mm00454586) and an 18S ribosomal RNA (rRNA) assay (ID Hs99999901). Real-time RT-PCR was performed with 10 ng total RNA on a sequence detection system (ABI Prism 7000; Applied Biosystems) with an RT-PCR system (SuperScript One-Step; Gibco BRL, Grand Island, NY). The threshold cycle of fluorescence units was evaluated to quantify mRNA levels, which were normalized according to the 18S rRNA levels and were expressed as the mean ± SD, as previously described.[20] Eyes with no laser injury were used as a control. The experiment was repeated three times.

Gelatin Zymography

At 3, 5, 9, and 21 days after laser injury (10 burns), the eyes were enucleated and analyzed by gelatin zymography using a commercially available electrophoresis kit (Gelatinzymo; Yagai Research Center, Yamagata, Japan), as previously described.[21] Briefly, equal amounts of protein (10 μg) were mixed with buffer (50 mM Tris-HCl buffer [pH 6.8] containing sodium dodecyl sulfate [SDS], glycerol, and bromophenol blue) and were electrophoresed. Supplied markers containing active MMP-2, pro-MMP-2, and pro-MMP-9 were also loaded onto the gel as references. After electrophoresis, the gels were agitated for 30 minutes in Triton X-100 buffer and shaken for 30 minutes in 50 mM Tris-HCl buffer (pH 7.5) containing NaCl to restore enzymatic activity. Samples were then incubated in 50 mM Tris-HCl buffer (pH 7.5) containing 200 mM NaCl and 5 mM $CaCl_2$ at 37°C for 26 hours to allow proteolysis of the gelatin. Subsequently, the gels were stained for 30 minutes with Coomassie blue and were destained in 30% methanol and 5% acetic acid. The experiment was repeated three times. Determination of the band intensity was analyzed by ImageJ software (developed by Wayne Rasband, National Institutes of Health, Bethesda, MD; available at http://rsb.info.nih.gov/ij/index.html), as previously described.[21]

Western Blot Analysis

At 1, 3, and 7 days after laser injury (10 burns), the eyes were enucleated, and the posterior segment of each was homogenized in radioimmunoprecipitation assay (RIPA) buffer. The homogenates were centrifuged at 20,000*g* for 15 minutes at 4°C, and the protein concentrations in the supernatants were determined using a DC protein assay kit (Bio-Rad Laboratories). Equal amounts of protein (10 μg/lane) were separated on 10% SDS-PAGE and electrophoretically transferred to polyvinylidene difluoride membranes. The membranes were blocked in Tris-buffered saline containing 0.1% Tween 20 and 5% bovine serum albumin and were incubated overnight at 4°C with 1:200 dilutions of primary antibody against mouse LOX-1, as previously described,[15] and then with a peroxidase-linked second antibody (Abcam, Cambridge, UK). Chemiluminescence was detected with an enhanced chemiluminescence Western blot analysis kit (Amersham Pharmacia Biotech). The experiment was repeated three times.

Enzyme-Linked Immunosorbent Assay for MCP-1 and VEGF

At 3 days after laser injury (15 burns), the eyes were enucleated and the RPE-choroid-sclera complex was isolated and homogenized in 250 μL RIPA buffer. Homogenates were centrifuged at 20,000*g* for 15 minutes at 4°C, and protein concentrations in the supernatants were determined as mentioned. MCP-1 and VEGF levels in the lysate were determined by a mouse MCP-1 or VEGF ELISA kit (R&D Systems, Minneapolis, MN) according to the manufacturer's protocol and were normalized to total protein as previously described.[22,23]

Incidence and Extension of Laser-Induced CNV

Incidences of CNV were determined by fluorescein angiography as previously described, with minor modifications.[19,24] At 14 days after laser injury (four burns), the lesions were studied by fluorescein angiography to evaluate CNV development and activity. Briefly, after intraperitoneal injection of 0.3 mL of 1% fluorescein sodium (Alcon, Tokyo, Japan), fluorescein angiography was performed at early and late phases using a scanning laser ophthalmoscope (SLO101; Rodenstock, Munich, Germany).

In addition, the mice were perfused with 20 mL phosphate-buffered saline (PBS) containing 50 μg/mL fluorescein-labeled tomato lectin (Vector Laboratories, Burlingame, CA) to stain the blood vessels. The eyes were harvested and fixed in 4% paraformaldehyde, and flatmounts of the RPE-choroid-sclera were prepared and stained for elastin using elastin ab (Sigma) followed by a Cy3-labeled secondary antibody (Sigma) as previously described.[25] The extent of laser-induced CNV was determined by confocal laser scanning microscopy as the area of fluorescein labeling in the flatmounts. Histologic images were captured, and pixels were measured using graphics software (Adobe Photoshop, version 7.0; Adobe Systems Inc., San Jose, CA) and ImageJ software (developed by Wayne Rasband, National Institutes of Health, Bethesda, MD; available at http://rsb.info.nih.gov/ij/index.html), according to the tutorial.

Statistical Analysis

Statistical comparisons of multiple groups were performed by one-way analysis of variance (ANOVA) followed by Fisher pairwise least significant difference (PLSD) test. Comparisons of two groups were made using either the χ^2 test or the Student *t*-test. $P < 0.05$ was considered statistically significant.

RESULTS

LOX-1 mRNA and Protein Expression in Laser-Induced CNV

Real-time RT-PCR analysis using total RNA derived from mouse retina-RPE-choroid-sclera tissue was performed to quantify the

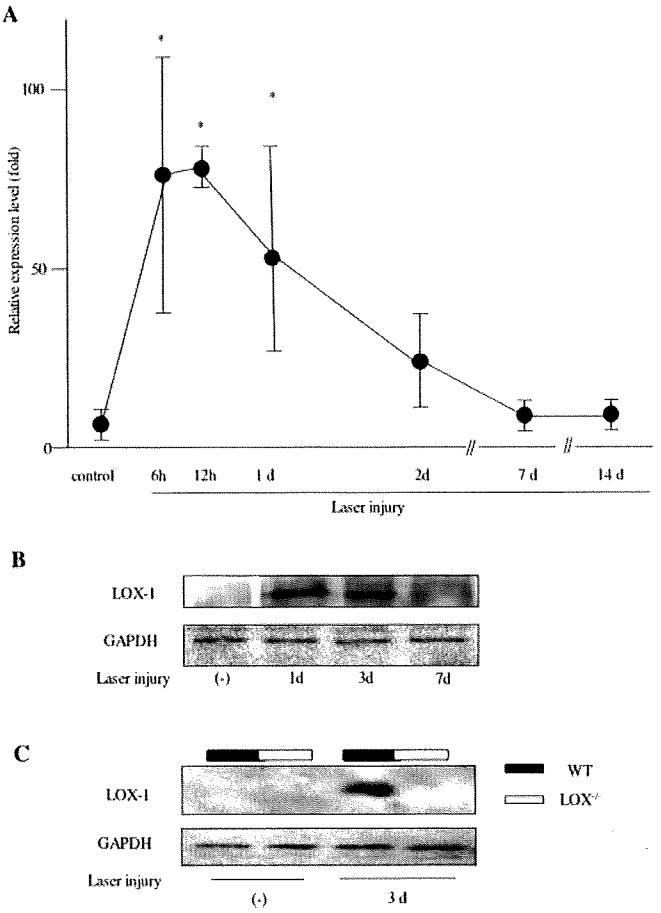

FIGURE 1. Real-time RT-PCR analysis of LOX-1 mRNA expression in posterior segment extract samples after laser injury (**A**). LOX-1 mRNA was standardized with 18S rRNA and expressed as the mean ± SD (n = 3). Data were analyzed using ANOVA. *Asterisks*: statistically significant differences ($P < 0.05$) compared with the control. Western blot analysis for LOX-1 in posterior segment extracts (**B**, **C**). LOX-1 expression was detected 1 day and 3 days after laser injury in wild-type mice (**B**). LOX-1 expression was not detected without laser injury in wild-type mice and LOX-1-deficient mice. The expression of LOX-1 was also not detected in LOX-1-deficient mice 3 days after laser injury (**C**). Glyceraldehyde-3-phosphate dehydrogenase (GAPDH) protein levels were included as a control.

relative levels of LOX-1 mRNA expression after laser injury. The expression level showed a transient peak between 6 and 12 hours after injury and then gradually returned to basal levels during the next 2 weeks (Fig. 1A). Semiquantitative analysis revealed that the relative expression of LOX-1 mRNA significantly increased 6 hours after laser injury by 71.5 ± 48.8-fold and peaked 12 hours after injury at 77.0 ± 7.7-fold compared with the control ($P = 0.011$ and $P = 0.0006$, respectively). At 1 day after injury, relative LOX-1 expression was significantly different from that of the control (52.8 ± 35.0-fold; $P = 0.01$). At 2, 7, and 14 days after injury, the relative LOX-1 expression was not significantly different from that of the control (32.2 ± 15.3-fold, $P = 0.09$; 6.7 ± 4.3-fold, $P = 0.75$; 6.8 ± 3.4-fold, $P = 0.74$, respectively). To confirm the expression of LOX-1 protein, Western blot analysis was performed. LOX-1 protein expression was clearly detected 1 day and 3 days after laser injury in wild-type mice (Fig. 1B) but was not detected in wild-type and LOX-1-deficient mice without laser injury. It also was not detected in LOX-1-deficient mice 3 days after laser injury (Fig. 1C).

Laser-Induced CNV in LOX-1–Deficient Mice

Our preliminary survey suggested that LOX-1-deficient mice undergo normal development of the ocular tissues and many organs, as observed previously.[15] Morphologic studies of LOX-1-deficient mouse eyes showed normal vasculature in the retinal and choroidal tissues and no abnormalities in the cornea, lens, iris, ciliary body (data not shown), and ocular fundus (Figs. 2A, B). To further determine the role of LOX-1, we compared the formation of laser-induced CNV between LOX-1-deficient and wild-type mice. At 14 days after laser injury, hematoxylin and eosin staining revealed proliferative membranes in the middle area of the lesion underlying the RPE and choroid in wild-type mice (Fig. 2C). By contrast, in LOX-1-deficient mice, fusiform membranes were rare and were primarily observed underlying the choroid (Fig. 2D).

Incidences of laser-induced CNV were determined by fluorescein angiography, which was performed 14 days after laser injury (Fig. 3). In wild-type mice, dye leakages, which were identified by the presence of hyper-fluorescein spots that became larger over time, were observed in 27 (93.0%) of the 29 burns. By contrast, dye leakage was significantly less common in LOX-1-deficient mice and was observed in 14 (58.3%) of the 24 burns ($P = 0.003$).

Perfusion of fluorescein-labeled tomato lectin was used to stain the vascular endothelium to measure the size of the laser-induced CNV, which was calculated from digitally captured images of RPE-choroid-sclera flat-mounts (Fig. 4A). The extent of CNV was significantly reduced in LOX-1-deficient mice compared with wild-type mice ($P = 0.011$; Fig. 4B), further confirming that laser-induced CNV was inhibited in LOX-1-deficient mice.

Induction and Activation of MMP-2 and MMP-9 Proteins

We next investigated the induction of MMP-2, pro-MMP-2, and pro-MMP-9 with gelatin zymography. In wild-type mice, the induction of pro-MMP-2 and pro-MMP-9 was clearly evident 3, 5, 9, and 21 days after laser injury (Fig. 5); the activated form of MMP-2 was also more conspicuous than basal level.

Similar experiments with LOX-1-deficient mice revealed only faint bands for MMP-2, pro-MMP-2, and pro-MMP-9. Densitometric analysis of the bands revealed that the induction of pro-MMP-9 in wild-type mice significantly increased 3 and 5 days after laser injury by 4.6 ± 1.3- and 4.6 ± 1.9-fold compared with the control ($P < 0.001$ and $P < 0.015$, respectively). The induction of pro-MMP-9 in LOX-1-deficient mice also increased 3 days after laser injury by 1.7 ± 0.5-fold compared with the control ($P = 0.022$).

There was a significant difference between wild-type mice and LOX-1-deficient mice with the induction of pro-MMP-9 at 3 and 5 days after laser injury ($P = 0.02$ and $P = 0.032$, respectively). In wild-type mice, the induction of pro-MMP-2 was significantly increased 3, 5, 9, and 21 days after laser injury by 14.7 ± 3.3-, 21.2 ± 5.2-, 16.6 ± 5.9-, and 13.4 ± 4.7-fold compared with the control, and the induction of MMP-2 was also increased 3, 5, 9, and 21 days after laser injury by 4.0 ± 1.0-, 5.4 ± 1.2-, 4.4 ± 0.7-, and 2.2 ± 1.0-fold compared with the control. By contrast, in LOX-1-deficient mice, the induction of pro-MMP-2 was increased 3, 5, and 9 days after laser injury by 8.4 ± 1.4, 6.7 ± 2.5-, and 5.9 ± 3.1-fold compared with the control, and the induction of MMP-2 also increased 3, 5, and 9 days after laser injury by 1.6 ± 0.5-, 2.9 ± 0.7-, and 2.9 ± 0.5-fold compared with the control. There was a significant difference between wild-type mice and LOX-1-deficient mice with the induction of pro-MMP-2 at 3, 5, 9, and 21 days after laser injury ($P = 0.04$, $P = 0.012$, $P = 0.05$, and $P = 0.044$, respectively), and there was a significant difference

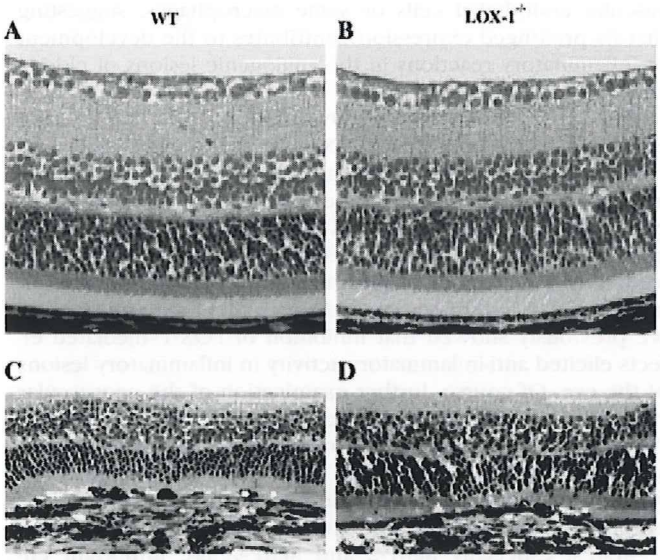

FIGURE 2. Histologic CNV sections in wild-type and LOX-1–deficient mice. Representative light micrographs of hematoxylin and eosin–stained sections of posterior segment in wild-type (**A**) and LOX-1–deficient (**B**) without laser injury and the middle of the CNV lesions in wild-type (**C**) and LOX-1–deficient (**D**) mice 14 days after laser injury. (**C**, **D**, *arrows*) Proliferative membranes. Scale bars, 50 μm.

between wild-type mice and LOX-1–deficient mice with the induction of MMP-2 at 3, 5, and 9 days after laser injury ($P = 0.021$, $P = 0.037$, and $P = 0.039$, respectively).

MCP-1 and VEGF Protein Expression

To identify and quantify MCP-1 and VEGF protein expression, we carried out ELISA of ocular tissue samples from eyes after laser injury (Fig. 6). The expression of MCP-1 protein was induced within 3 days of laser treatment in wild-type eyes and then gradually returned to basal levels by Western blot analysis (data not shown). Therefore, we detected MCP-1 protein expression 3 days after laser injury by ELISA. MCP-1 was not detected in wild-type mice or LOX-1–deficient mice without laser injury, and it increased in wild-type mice 3 days after laser injury (110.7 ± 38.1 pg/mg protein). MCP-1 protein expression in LOX-1–deficient mice (63.4 ± 14.2 pg/mg protein) was significantly decreased compared with wild-type mice ($P = 0.014$). Previous reports demonstrated that VEGF concentrations peaked at 3 days after laser injury.[22,23] Accordingly, we examined VEGF protein expression 3 days after laser injury by ELISA. Without laser injury, VEGF protein expression was not significantly different between wild-type mice (16.1 ± 5.2 pg/mg protein) and LOX-1–deficient mice (20.2 ± 11.3 pg/mg protein). Although VEGF protein expression was clearly increased in wild-type mice (121.3 ± 18.2 pg/mg protein) 3 days after laser injury, the increasing level was markedly decreased in LOX-1–deficient mice (93.4 ± 13.1 pg/mg protein; $P = 0.032$).

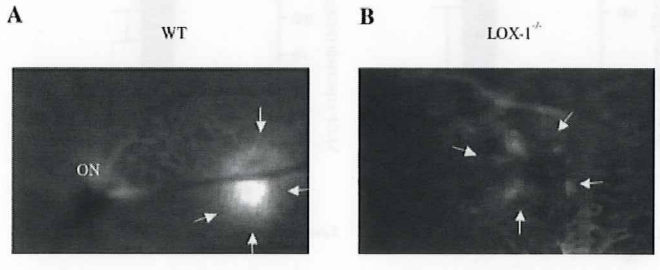

C

Mice	N	Fluorescein leakage
Wild type	29	27 (93.1%)
LOX-1 deficient	24	14 (58.3%)

FIGURE 3. Representative images of the late stage of fluorescein angiography 14 days after laser injury in wild-type (**A**) and LOX-1–deficient (**B**) mice. (**C**) Fluorescein leakage-spot data in wild-type (eight eyes) and LOX-1–deficient (six eyes) mice. *Arrows*: leakage points. ON, optic nerve.

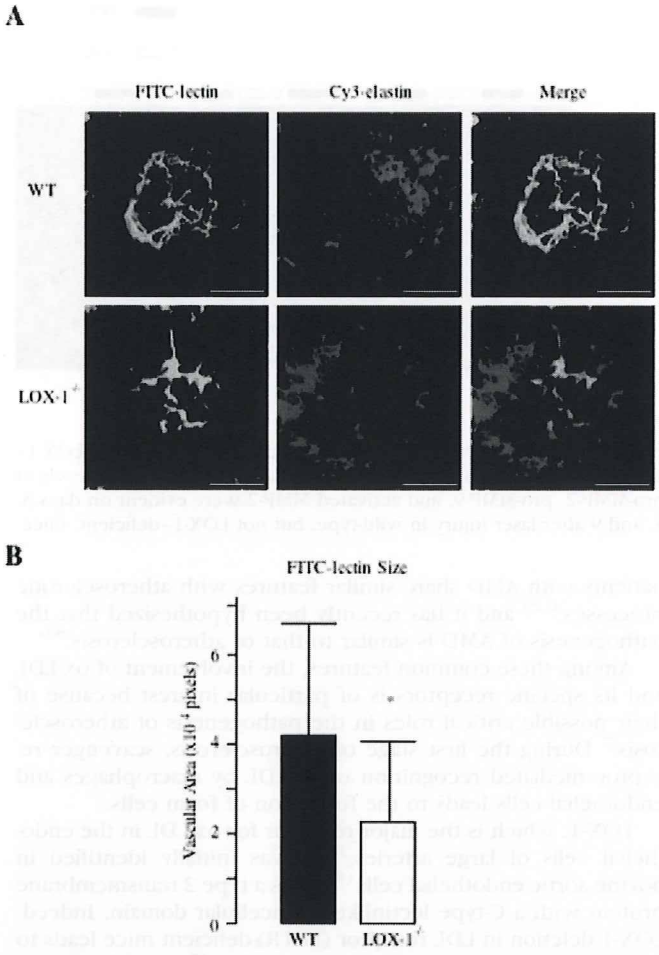

FIGURE 4. (**A**) Representative micrographs of CNV lesions 14 days after laser injury, stained with fluorescein isothiocyanate (FITC)-lectin (*left*) and Cy3-labeled elastin (*middle*) in wild-type mice (*upper*) and LOX-1–deficient mice (*lower*). Scale bars, 50 μm. (**B**) Computer image analysis revealed a significantly smaller CNV area in LOX-1–deficient mice (four eyes) than in wild-type mice (four eyes). *Asterisks*: statistically significant differences ($P = 0.011$). Absolute values were as follows: $n = 12$ and mean ± SD = $4.27 \pm 2.58 \times 10^4$ pixels for wild-type mice; $n = 12$ and mean ± SD = $2.46 \pm 1.63 \times 10^4$ pixels for LOX-1–deficient mice.

DISCUSSION

Numerous factors, including oxidative stress, inflammatory reactions (such as complement activation), upregulated chemokines, and remodeling in the extracellular matrices, are involved in the pathogenesis of CNV in eyes with AMD.[25–28] Earlier studies have demonstrated that the drusen and CNVs of

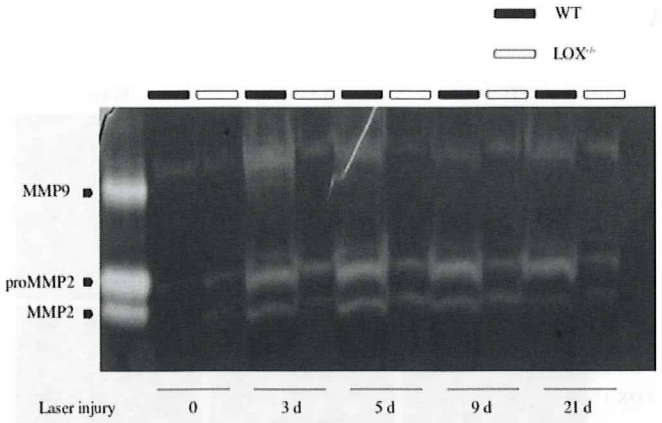

FIGURE 5. Gelatin zymography of wild-type (*black bars*) and LOX-1-deficient (*white bars*) mouse eyes after laser injury. Increased levels of pro-MMP-2, pro-MMP-9, and activated MMP-2 were evident on days 3, 5, and 9 after laser injury in wild-type, but not LOX-1-deficient, mice.

patients with AMD share similar features with atherosclerotic processes,[6,29] and it has recently been hypothesized that the pathogenesis of AMD is similar to that of atherosclerosis.[5,6]

Among these common features, the involvement of ox-LDL and its specific receptors is of particular interest because of their possible critical roles in the pathogenesis of atherosclerosis.[7] During the first stage of atherosclerosis, scavenger receptor–mediated recognition of ox-LDL by macrophages and endothelial cells leads to the formation of foam cells.

LOX-1, which is the major receptor for ox-LDL in the endothelial cells of large arteries,[30,31] was initially identified in bovine aortic endothelial cells[14] and is a type 2 transmembrane protein with a C-type lectinlike extracellular domain. Indeed, LOX-1 deletion in LDL receptor (LDLR)-deficient mice leads to reduced atherogenesis formation in vivo.[15] Previously, we showed that LOX-1 is expressed in surgically obtained CNV specimens.[16] From this observation, we hypothesized that LOX-1 is involved in the pathogenesis of CNV formation and that elucidation of the molecular basis of its contribution to angiogenic lesions in the ocular fundus might lead to novel therapeutic concepts.

In the present study, real-time RT-PCR revealed the upregulated expression of LOX-1 mRNA in the acute phase after laser injury to the retina. We were also able to detect the upregulated expression of LOX-1 protein by laser injury in Western blot analysis, but we were unable to localize the upregulated expression of LOX-1 in immunohistochemistry. Previous investigations have suggested that a number of factors can induce LOX-1 expression under inflammatory conditions. For example, LOX-1 can be immediately induced by proinflammatory stimulants, such as the presence of oxidant species,[32] cytokines,[33] and shear stress,[34] suggesting that it is an immediate-early gene. Our results are in accordance with these findings because laser injury causes the induction of proinflammatory cytokines in the injured region.

Upregulated LOX-1 expression has also been indicated in inflammatory changes of the vascular endothelium through the generation of superoxide,[35] the reduction of nitric oxide,[36] the induction of MCP-1,[18] and the promotion of leukocyte adhesion.[37] We previously observed that the inhibition of LOX-1–mediated effects greatly decreased the inflammatory reaction of animal eyes by reducing the adhesion between circulating leukocytes and retinal vascular endothelial cells.[37] Therefore, we concluded that LOX-1 is a deteriorating factor in retinal and/or choroid inflammatory reactions as part of a cascade. However, previous studies (including our own) of clinical human CNV samples have demonstrated LOX-1 expression in vascular endothelial cells or some macrophages, suggesting that its prolonged expression contributes to the development of inflammatory reactions in the angiogenic lesions of elderly patients.

The present study revealed that the formation of CNV after laser injury is inhibited in LOX-1-deficient mice. This was confirmed by fluorescein angiography and lectin staining and implied that LOX-1 plays an important role in the pathogenesis of CNV lesions. Given that LOX-1 is involved in many inflammatory reactions of diseased tissues, its reduced expression leading to a deficiency of inflammation would inhibit the formation of CNV after laser injury. In agreement with this theory, we previously showed that inhibition of LOX-1–mediated effects elicited anti-inflammatory activity in inflammatory lesions of the eye. Of course, further examination of the neovascular response with the use of antiserum to block the function of LOX-1 will be required to confirm our hypothesis. Our present study of the LOX-1 effect on MMP and MCP-1 expression further investigated this hypothesis, with particular emphasis on proinflammatory cytokines and related enzymes.

MMPs, especially MMP-2 and MMP-9, are important enzymes for vascular remodeling in many disorders, and their levels are increased in human CNVs with exudative AMD. Mice that were doubly deficient for MMP-2 and MMP-9 demonstrated attenuated CNV in terms of incidence and severity compared with single gene-deficient mice or corresponding wild-type controls. From these findings, it was deduced that MMP-2 and MMP-9 might cooperate in the development of AMD[10] It has also been shown that reduced CNV formation occurs in MMP-2-deficient mice.[38] Our results suggest that a deletion of LOX-1 inhibits the induction pro-MMP-2 and pro-MMP-9 and the activation of MMP-2 after laser injury.

Some previous studies have found that MMP-9 microsatellite polymorphisms are associated with susceptibility to the exudative form of AMD,[39] whereas others have described elevated levels of MMP-9 in the plasma of patients with AMD.[40] Hence, there is increasing evidence for the critical involvement of

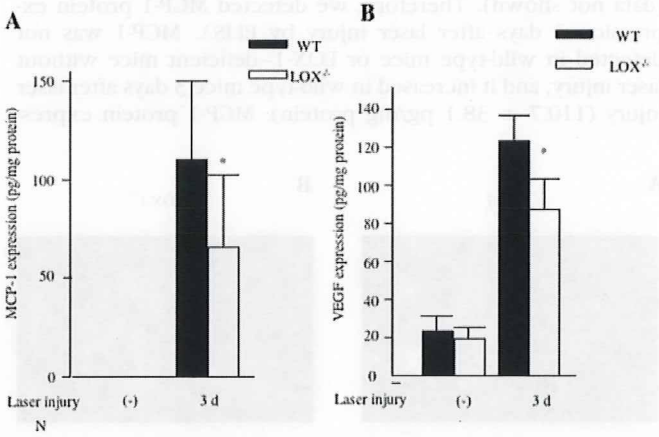

FIGURE 6. Assessment of MCP-1 and VEGF levels in eyes from wild-type (*black bars*) and LOX-1-deficient (*white bars*) mice after laser injury. MCP-1 (**A**) and VEGF (**B**) protein expression were measured by ELISA in eyes from wild-type (*black bars*) and LOX-1-deficient (*white bars*) mice without laser injury and 3 days after laser injury. MCP-1 protein expression was not detected in wild-type mice or LOX-1-deficient mice ($n = 5$ and $n = 4$, respectively). The concentrations of MCP-1 protein were 110.7 ± 38.1 in wild-type mice and 63.4 ± 14.2 in LOX-1-deficient mice ($n = 12$ and $n = 6$, respectively) 3 days after laser injury. The concentration of VEGF protein was 16.1 ± 5.2 in wild-type mice and 20.2 ± 11.3 in LOX-1-deficient mice without laser injury ($n = 5$ and $n = 4$, respectively). Three days after laser injury, the concentration of VEGF protein was 121.3 ± 18.2 in wild-type mice and 93.4 ± 13.1 in LOX-1-deficient mice ($n = 8$ and $n = 8$, respectively).

MMPs and the resultant remodeling of extracellular matrices in the pathogenesis of CNV. Our zymographic experiments indicated that the molecular mechanisms of LOX-1, in relation to CNV formation, might be elicited by the regulation of MMP-2 and MMP-9.

Activations of LOX-1 and MCP-1 were also demonstrated to be collectively involved in the early stages of atherosclerosis in hypertensive rats.[41] Our animal experiments revealed that the deletion of LOX-1 inhibited the expression of MCP-1 after laser injury. MCP-1 is well known to play as an important molecule in monocyte recruitment and angiogenic processes. Previous studies reported that MCP-1 is a key factor for the formation of CNV after laser injury.[42,43] Our finding suggested that the involvement of MCP-1 in CNV membranes has been demonstrated in clinical and experimental samples, in agreement with our findings.[13,43,44]

Using a specific antisense to human LOX-1 mRNA, the receptor has been shown to be a key factor in regulating the expression of MCP-1 and ox-LDL–mediated monocyte adhesion to vascular endothelial cells.[18] On the other hand, LOX-1–dependent redox signal pathways have been shown to promote the expression of VEGF induced by angiotensin II and the expression of MMPs induced by ox-LDL in endothelial cells.[17,45] These findings propose a hypothesis that the LOX-1–mediated redox signal pathway, including mitogen-activated protein kinase, is a crucial factor for angiogenesis mediated by MCP-1, VEGF, and MMPs. Our present study indicated that the activation of MMPs and the expression of MCP-1 and VEGF by laser injury were suppressed in LOX-1–deficient mice compared with wild-type mice. However, we could not examine the development of CNV at various time points and assay the expression of LOX-1, VEGF, MCP-1, and MMPs at the same time points in this study because we determined the time points based on previous reports[10,13,19,23] and the LOX-1–deficient mice were limited. Based on our finding, the relationships among LOX-1, MCP-1, VEGF, and MMPs were not clarified in the development of CNV. Therefore, further studies will be required to fully elucidate these relationships and the complicated network of AMD pathogenesis.

In conclusion, the present study shows that upregulated expression of LOX-1 can be induced by laser injury. Our results clearly indicate, for the first time, the involvement of LOX-1 and associated factors in the formation and deterioration of CNV. Although further studies will be needed to clarify the significance of LOX-1 in the pathogenesis of AMD, this work suggests that the inhibition of SRs could be a novel therapeutic modality for AMD.

References

1. Fine SL, Berger JW, Maguire MG, Ho AC. Age-related macular degeneration. *N Engl J Med.* 2000;342(7):483–492.
2. Haines JL, Hauser MA, Schmidt S, et al. Complement factor H variant increases the risk of age-related macular degeneration. *Science.* 2005;308(5720):419–421.
3. Vingerling JR, Hofman A, Grobbee DE, de Jong PT. Age-related macular degeneration and smoking: the Rotterdam Study. *Arch Ophthalmol.* 1996;114(10):1193–1196.
4. McGwin G Jr, Xie A, Owsley C. The use of cholesterol-lowering medications and age-related macular degeneration. *Ophthalmology.* 2005;112(3):488–494.
5. Friedman E. The role of the atherosclerotic process in the pathogenesis of age-related macular degeneration. *Am J Ophthalmol.* 2000;130(5):658–663.
6. Mullins RF, Russell SR, Anderson DH, Hageman GS. Drusen associated with aging and age-related macular degeneration contain proteins common to extracellular deposits associated with atherosclerosis, elastosis, amyloidosis, and dense deposit disease. *FASEB J.* 2000;14(7):835–846.
7. Ross R. Atherosclerosis-an inflammatory disease. *N Engl J Med.* 1999;340(2):115–126.
8. Ikeda T, Obayashi H, Hasegawa G, et al. Paraoxonase gene polymorphisms and plasma oxidized low-density lipoprotein level as possible risk factors for exudative age-related macular degeneration. *Am J Ophthalmol.* 2001;132(2):191–195.
9. Kamei M, Yoneda K, Kume N, et al. Scavenger receptors for oxidized lipoprotein in age-related macular degeneration. *Invest Ophthalmol Vis Sci.* 2007;48(4):1801–1807.
10. Lambert V, Wielockx B, Munaut C, et al. MMP-2 and MMP-9 synergize in promoting choroidal neovascularization. *FASEB J.* 2003;17(15):2290–2292.
11. Sluijter JP, de Kleijn DP, Pasterkamp G. Vascular remodeling and protease inhibition: bench to bedside. *Cardiovasc Res.* 2006; 69(3):595–603.
12. Cheng C, Tempel D, van Haperen R, et al. Shear stress-induced changes in atherosclerotic plaque composition are modulated by chemokines. *J Clin Invest.* 2007;117(3):616–626.
13. Nagai N, Oike Y, Izumi-Nagai K, et al. Suppression of choroidal neovascularization by inhibiting angiotensin-converting enzyme: minimal role of bradykinin. *Invest Ophthalmol Vis Sci.* 2007;48(5): 2321–2326.
14. Sawamura T, Kume N, Aoyama T, et al. An endothelial receptor for oxidized low-density lipoprotein. *Nature.* 1997;386(6620):73–77.
15. Mehta JL, Sanada N, Hu CP, et al. Deletion of LOX-1 reduces atherogenesis in LDLR knockout mice fed high cholesterol diet. *Circ Res.* 2007;100(11):1634–1642.
16. Honjo M, Sawamura T, Hinagata J, et al. Expression of LOX-1, an oxidized low-density lipoprotein receptor, in choroidal neovascularization. *Arch Ophthalmol.* 2004;122(12):1873–1876.
17. Li D, Liu L, Chen H, et al. LOX-1 mediates oxidized low-density lipoprotein-induced expression of matrix metalloproteinases in human coronary artery endothelial cells. *Circulation.* 2003;107(4): 612–617.
18. Li D, Mehta JL. Antisense to LOX-1 inhibits oxidized LDL-mediated upregulation of monocyte chemoattractant protein-1 and monocyte adhesion to human coronary artery endothelial cells. *Circulation.* 2000;101(25):2889–2895.
19. Tobe T, Ortega S, Luna JD, et al. Targeted disruption of the FGF2 gene does not prevent choroidal neovascularization in a murine model. *Am J Pathol.* 1998;153(5):1641–1646.
20. Awai M, Koga T, Inomata Y, et al. NMDA-induced retinal injury is mediated by an endoplasmic reticulum stress-related protein, CHOP/GADD153. *J Neurochem.* 2006;96(1):43–52.
21. Takano A, Hirata A, Inomata Y, et al. Intravitreal plasmin injection activates endogenous matrix metalloproteinase-2 in rabbit and human vitreous. *Am J Ophthalmol.* 2005;140(3):654–660.
22. Sakurai E, Anand A, Ambati BK, van Rooijen N, Ambati J. Macrophage depletion inhibits experimental choroidal neovascularization. *Invest Ophthalmol Vis Sci.* 2003;44:3578–3585.
23. Itaya M, Sakurai E, Nozaki M, et al. Upregulation of VEGF in murine retina via monocyte recruitment after retinal scatter laser photocoagulation. *Invest Ophthalmol Vis Sci.* 2007;48:5677–5683.
24. Sagara N, Kawaji T, Takano A, et al. Effect of pitavastatin on experimental choroidal neovascularization in rats. *Exp Eye Res.* 2007;84(6):1074–1080.
25. Bora PS, Sohn JH, Cruz JM, et al. Role of complement and complement membrane attack complex in laser-induced choroidal neovascularization. *J Immunol.* 2005;174(1):491–497.
26. Schlingemann RO. Role of growth factors and the wound healing response in age-related macular degeneration. *Graefes Arch Clin Exp Ophthalmol.* 2004;242(1):91–101.
27. Campochiaro PA, Soloway P, Ryan SJ, Miller JW. The pathogenesis of choroidal neovascularization in patients with age-related macular degeneration. *Mol Vis.* 1999;5:34.
28. Lopez PF, Sippy BD, Lambert HM, Thach AB, Hinton DR. Transdifferentiated retinal pigment epithelial cells are immunoreactive for vascular endothelial growth factor in surgically excised age-related macular degeneration-related choroidal neovascular membranes. *Invest Ophthalmol Vis Sci.* 1996;37(5):855–868.
29. Lopez PF, Grossniklaus HE, Lambert HM, et al. Pathologic features of surgically excised subretinal neovascular membranes in age-

related macular degeneration. *Am J Ophthalmol.* 1991;112(6):647–656.

30. Kume N, Moriwaki H, Kataoka H, et al. Inducible expression of LOX-1, a novel receptor for oxidized LDL, in macrophages and vascular smooth muscle cells. *Ann N Y Acad Sci.* 2000;902:323–327.
31. Nagase M, Ando K, Nagase T, et al. Redox-sensitive regulation of LOX-1 gene expression in vascular endothelium. *Biochem Biophys Res Commun.* 2001;281(3):720–725.
32. Li D, Mehta JL. Upregulation of endothelial receptor for oxidized LDL (LOX-1) by oxidized LDL and implications in apoptosis of human coronary artery endothelial cells: evidence from use of antisense LOX-1 mRNA and chemical inhibitors. *Arterioscler Thromb Vasc Biol.* 2000;20(4):1116–1122.
33. Kume N, Murase T, Moriwaki H, et al. Inducible expression of lectin-like oxidized LDL receptor-1 in vascular endothelial cells. *Circ Res.* 1998;83(3):322–327.
34. Murase T, Kume N, Korenaga R, et al. Fluid shear stress transcriptionally induces lectin-like oxidized LDL receptor-1 in vascular endothelial cells. *Circ Res.* 1998;83(3):328–333.
35. Cominacini L, Pasini AF, Garbin U, et al. Oxidized low density lipoprotein (ox-LDL) binding to ox-LDL receptor-1 in endothelial cells induces the activation of NF-κB through an increased production of intracellular reactive oxygen species. *J Biol Chem.* 2000;275(17):12633–12638.
36. Cominacini L, Rigoni A, Pasini AF, et al. The binding of oxidized low density lipoprotein (ox-LDL) to ox-LDL receptor-1 reduces the intracellular concentration of nitric oxide in endothelial cells through an increased production of superoxide. *J Biol Chem.* 2001;276(17):13750–13755.
37. Honjo M, Nakamura K, Yamashiro K, et al. Lectin-like oxidized LDL receptor-1 is a cell-adhesion molecule involved in endotoxin-induced inflammation. *Proc Natl Acad Sci U S A.* 2003;100(3):1274–1279.
38. Berglin L, Sarman S, van der Ploeg I, et al. Reduced choroidal neovascular membrane formation in matrix metalloproteinase-2-deficient mice. *Invest Ophthalmol Vis Sci.* 2003;44(1):403–408.
39. Fiotti N, Pedio M, Battaglia Parodi M, et al. MMP-9 microsatellite polymorphism and susceptibility to exudative form of age-related macular degeneration. *Genet Med.* 2005;7(4):272–277.
40. Chau KY, Sivaprasad S, Patel N, et al. Plasma levels of matrix metalloproteinase-2 and -9 (MMP-2 and MMP-9) in age-related macular degeneration. *Eye.* 2008;22(6):855–859.
41. Hamakawa Y, Omori N, Ouchida M, et al. Severity dependent upregulations of LOX-1 and MCP-1 in early sclerotic changes of common carotid arteries in spontaneously hypertensive rats. *Neurol Res.* 2004;26(7):767–773.
42. Yamada K, Sakurai E, Itaya M, Yamasaki S, Ogura Y. Inhibition of laser-induced choroidal neovascularization by atorvastatin by downregulation of monocyte chemotactic protein-1 synthesis in mice. *Invest Ophthalmol Vis Sci.* 2007;48(4):1839–1843.
43. Grossniklaus HE, Ling JX, Wallace TM, et al. Macrophage and retinal pigment epithelium expression of angiogenic cytokines in choroidal neovascularization. *Mol Vis.* 2002;8:119–126.
44. Tsutsumi C, Sonoda KH, Egashira K, et al. The critical role of ocular-infiltrating macrophages in the development of choroidal neovascularization. *J Leukoc Biol.* 2003;74(1):25–32.
45. Hu C, Dandapat A. Mehta JL. Angiotensin II induces capillary formation from endothelial cells via the lox-1–dependent redox-sensitive pathway. *Hypertension.* 2007;50:952–957.

LOX-1
—— The Multifunctional Receptor Underlying Cardiovascular Dysfunction ——

Sayoko Ogura, MD; Akemi Kakino, MS; Yuko Sato, PhD;
Yoshiko Fujita, PhD; Shin Iwamoto, MS; Kazunori Otsui, MD;
Ryo Yoshimoto, PhD; Tatsuya Sawamura, MD

Oxidatively modified low-density lipoprotein (oxLDL) is implicated in the pathogenesis of atherosclerosis. Endothelial dysfunction is the initial change in the vascular wall that induces morphological changes for atheroma-formation. Lectin-like oxidized LDL receptor-1 (LOX-1) was identified as the receptor for oxLDL that was thought to be a major cause of endothelial dysfunction. LOX-1 has been demonstrated to contribute not only to endothelial dysfunction, but also to atherosclerotic-plaque formation, myocardial infarction and intimal thickening after balloon injury. Recent findings on the genetics of LOX-1 and the methodology to detect it and its ligands would further facilitate the examination of the receptor's pathophysiological contribution in atherosclerosis. Furthermore, LOX-1-related tools might open new gateways from diagnosis to therapeutics for cardiovascular diseases.

Key Words: Atherosclerosis; Endothelial dysfunction; LOX-1; Oxidized low-density lipoprotein

Atherosclerosis is characterized by the accumulation of lipids and fibrous elements in the arteries, and is the most important contributor to the growing burden of cardiovascular diseases. The major risk factors of atherosclerosis, such as hypertension, diabetes, smoking and free radicals, have been known to induce endothelial dysfunction.[1,2] Endothelial dysfunction, functional changes in endothelial cells, has been thought to precede morphological changes of atheroma.[1] Lectin-like oxidized low density lipoprotein receptor-1 (LOX-1) was identified from endothelial cells as the molecule that induces endothelial dysfunction triggered by oxidized low-density lipoprotein (LDL).[3] LOX-1 is a 50 kDa type II transmembrane glycoprotein comprising 273 amino acids.[3] The protein contains a short N-terminal cytoplasmic domain, a single transmembrane domain and an extracellular domain comprising a neck domain followed by a C-terminal C-type lectin-like ligand-binding domain (**Figure 1**).[4] LOX-1 has been demonstrated to actively contribute to all stages of atherogenesis. LOX-1 is expressed not only in endothelial cells, but also in macrophages,[5] vascular smooth muscle cells[6] and platelets.[7] In vitro, the basal expression of LOX-1 in endothelial cells is limited; however, it can be rapidly induced by pro-inflammatory, pro-oxidative and mechanical stimuli.[8–14] In vivo, the basal expression of LOX-1 is also low, but can be enhanced by several pathological conditions, including hypertension,[15] diabetes mellitus,[16] hyperlipidemia[17] and chronic renal failure.[18] Here, we aim to briefly review the roles of LOX-1 in various diseases to understand the vascular, as well as myocardial, LOX-1 function in basic and clinical medicine.

LOX-1 Signaling

Oxidative modification of LDL (oxLDL) has been known to increase its atherogenecity.[19] Several reports have revealed that elevated plasma levels of oxLDL are associated with coronary artery diseases (CAD).[20] The plasma levels of oxLDL are related to the presence of angiographically detected complex and thrombotic lesion morphology in patients with unstable angina.[21] LOX-1 binding to oxLDL enhances nitric oxide (NO) catabolism as a result of superoxide generation, and decreases NO release via attenuated endothelial NO synthase (eNOS) activity. LOX-1 has been recently shown to form a complex with MT1-MMP under a basal condition.[22] When oxLDL binds to LOX-1 it induces rapid RhoA and Rac1 activation via MT1-MMP, which results in NADPH oxidase activation and eNOS down-regulation.[22] The imbalance of NO and oxidative stress resulting from the binding of oxLDL to LOX-1 causes oxLDL-induced endothelial dysfunction leading to atherosclerosis.

In addition to the Rho and Rac pathways, the following signal transduction pathways have been reported to be activated via LOX-1: p38 mitogen-activated protein kinase C (MAPK),[23,24] p44/42MAPK,[11] protein kinase C,[25] protein kinase B,[26] ERK1/2,[27] protein tyrosine kinase[28] and NF-κB. Among them, LOX-1-mediated NF-κB activation by oxLDL is crucial for increasing the expressions of the following adhesion molecules: E- and P-selectins, intracellular adhe-

Received August 11, 2009; accepted August 26, 2009; released online October 5, 2009
Department of Vascular Physiology, National Cardiovascular Center, Suita, Japan
Mailing address: Tatsuya Sawamura, MD, Department of Vascular Physiology, National Cardiovascular Center, 5-7-1 Fujishirodai, Suita 565-8565, Japan. E-mail: t-sawamura@umin.ac.jp